FINAL REPORT

NASA LANGLEY RESEARCH CENTER

P-61

CONTRACT #NAG-1-1157

A. VELOCITY PROFILES IN A HOT JET BY SIMPLIFIED RELIEF

B. THE APPLICATION OF THE RELIEF TECHNIQUE FOR VELOCITY FIELD MEASUREMENTS IN THE ASTF-C1 TEST CELL

Richard B. Miles
Principal Investigator

Walter R. Lempert
Co-Principal Investigator

Work Period: 6/12/90 to 6/30/91

November 15, 1991

TABLE OF CONTENTS

CONTRACT NAG-1-1157

FINAL REPORT FOR NASA-LANGLEY CONTRACT #NAG-1-1157

A. "VELOCITY PROFILES IN A HOT JET BY SIMPLIFIED RELIEF"

Attn: G.B. Northam, Experimental Methods Branch
MS 168
NASA Langley Research Center
Hampton, VA 23665

INTRODUCTION

The principal goal of this research effort has been to provide support for the installation of simplified RELIEF (1) flow tagging instrumentation at NASA-Langley Research Center. RELIEF is a double resonance velocimetry technique in which oxygen molecules are vibrationally excited via stimulated Raman scattering at a specific location within a flow field. After suitable time delay, typically 1-10 microseconds, the displacement of the tagged molecules is determined by laser-induced fluorescence imaging.

The current work has centered around characterization and optimization of a high-pressure O_2 stimulated Raman cell, which greatly simplifies the tagging step. During the work period, conversion efficiency and spectral profile measurements have been performed under a variety of conditions, and a 2 m long cell has been installed at NASA-Langley. Additionally, limited work has been performed on improvements to a high-intensity, ultraviolet flashlamp, which was used, for the first time, to obtain images of vibrationally excited oxygen in a low-speed O_2 jet. The ultimate goal of this part of the effort is to find a substitute for the argon-fluoride laser which is currently used for the laser-induced fluorescence interrogation step.

REVIEW OF WORK PERFORMED

A. Characterization of Stimulated Raman Cell

1. Conversion Efficiency

The vibrational tagging step requires two high power laser beams with frequency difference equal to the vibrational frequency of oxygen. In the original RELIEF experiments, the second laser beam was derived from the first using a dye laser. This required that the primary laser beam be split into two parts, one of which pumped the dye laser and, subsequently, that the two beams be recombined. The two laser beams had to be overlapped in time, space, and frequency, and the primary beam had to be powerful enough to pump the dye laser, which is not a particularly efficient process. Recently (2), we have developed a high pressure O_2 stimulated Raman cell which directly converts a portion of the primary beam to the desired second wavelength. The two beams exit the cell automatically matched in frequency and time, and with excellent spatial overlap.

In the last year, we have worked to optimize the Raman cell conditions by studying a variety of configurations. The results of these studies are summarized in Table I. As can be seen, three different cells have been examined. The first is a rather conventional 2 m long cell, which has been studied with a variety of focusing lenses in both single and double-pass modes. The second is a 6 m long cell, and the third is a 1 m long, cylindrical optics, multi-pass cell. We will now discuss these cells in more detail.

a. **2-Meter Cell**

The 2 m cell has been studied in most detail because it is the simplest to both construct and to use in common laboratory environments. It has been determined that an approximately 1:1 mixture of O_2:He at 1000 psi total pressure is an optimum gas mixture for Q-switched YAG lasers with 250-300 mJ/pulse energy operating at 5-10 Hz repetition rate. The helium buffer serves to diffuse heat which is built-up along the beam waist due to the vibrational excitation which occurs as part of the conversion process. The total pressure must be fairly high because the Raman gain of oxygen is relatively low (less than 1/100th of H_2, for example, at STP).

Figure 1 shows 1st Stokes conversion efficiency (•) and fractional loss (o) as a function of input laser energy for 1.0, 1.5, and 2.0 m focal length focusing lenses, using the 2 m cell with a 450:550 psi O_2:He mixture. All data is taken using the second harmonic of a Nd:YAG laser at 0.532 microns, with ~10 nsec pulse duration and a repetition rate of 10 Hz. As discussed in Reference 2, the laser is operated in its broad-band mode which results in a linewidth of ~1 cm^{-1}. This, combined with a relatively long confocal beam parameter, serves to suppress stimulated Brillouin backscatter (SBS) which competes with the Raman conversion. As can be seen, use of the 1 m focal length lenses results in significant SBS energy loss (~60%) for all but the lowest input pulse energies. The corresponding conversion efficiency ranges from <1% at 65 mj/pulse to ~5% at 350 mJ/pulse. Increasing the focal length of the focusing lens to 1.5 m results in an increase in the conversion efficiency to ~8-9%, and a drop in the energy loss to ~20%. This configuration, with ~250-300 mJ of input energy is now

b. Other Cells

Limited experiments have been performed with a 6 m cell which was constructed by bolting three 2 m segments together, and a cylindrical multi-pass cell, based on an optical configuration used by Long, et al. (3) for increasing the sensitivity of Rayleigh scattering measurements. The 6 m cell, despite being certified to only 600 psi total pressure, gave a single-pass conversion using a 4 m focal length input lens in the 11-12% range. The SBS loss was negligible. The cylindrical cell gave the highest conversion efficiency (~30%) of all the cells used, but the repetition rate was limited to 1 Hz. The windows of this cell are 2" (~1-1/2" unsupported), so that the total working pressure is limited to 500 psi. Due to the multi-pass arrangement and the cylindrical focusing, thermal beam degradation is more significant in this cell, resulting in the low repetition rate. (It is anticipated that increasing the helium buffer partial pressure would result in some improvement.)

2. Pressure-Shifting Measurements

At the high pressures required for operation of the O_2 Raman cell, it is important to verify that the 1st Stokes frequency overlaps with that corresponding to O_2 at near 1 atm conditions. In order to verify this, we have performed simple scanning coherent anti-Stokes Raman spectroscopy (CARS) Q-branch measurements in the high-pressure cell and ordinary room air, simultaneously. As discussed in Reference 2, at high pressure, the individual rotational lines within the vibrational Q-branch merge into one feature. The results of these measurements are summarized in Figs. 3a and

3b. From Fig. 3a, which corresponds to pure O_2 at 450 psi, the high-pressure Q-branch overlaps almost perfectly with the J=7 transition at room conditions. In the 450:550 psi O_2:He mixture of Fig. 3b, the high-pressure Q-branch has shifted slightly (~0.3 cm^{-1}) and now peaks approximately midway between the J=7 and J=9 transitions at room conditions. Since the Nd:YAG pump beam has a spectral width of ~1 cm^{-1}, these results indicate that the 1st Stokes output from the cell should efficiently pump oxygen molecules in the J=7 and J=9 rotational levels.

B. Ultra-Violet Flashlamp Development

We have performed some limited additional work on the development of a high brightness, ultraviolet flashlamp for use as a flow interrogation source. A schematic of an earlier lamp design is shown in Fig. 4. The lamp, based upon a design of Holzrichter and Emmett (4), is a windowless, coaxial discharge lamp which uses flowing helium gas. In a prior reporting period (5), we measured the spectral and spatial light output of the lamp and obtained an estimated effective blackbody temperature of ~25,000 K.

During this work period, it was determined that a significant amount of energy was dissipated across the spark gap, and that the spark gap was also a significant source of inductance. Removal of the spark gap resulted in a decrease in the pulse duration, and a large increase in the UV pulse energy. In the last report, a pulse energy of 0.06 mJ (in an ~10 nm spectral band centered at 185 nm), and a pulse duration of ~12 microseconds was obtained using a 2 μF capacitor and 8 KV charging voltage with helium flow gas. Upon removal of the spark gap, using a 5 F capacitor and a 5-6 KV charging

voltage, the pulse duration was reduced to ~5 microseconds, and the UV pulse energy in the same band was increased to greater than 1 mJ/pulse. These pulse energies are measured with a pyroelectric joulemeter, purchased with previous funding for this research. The energies represent net numbers, obtained by subtraction of measured energies without nitrogen pumping of the optical system, from measured energies including purging. The spectral filtering of the very broad band lamp output is performed with a pair of ArF lasers 193 nm high reflectors tilted off-axis to shift the peak of the reflectivity. This is illustrated in Fig. 5, which shows the optical configuration and the measurement location. Figure 6 shows the resulting spectral band.

Spectral scans were performed using the optical set-up of Fig. 5, but with a purgable spectrometer in place of the joulemeter. Figure 7 shows two traces, the upper being with a nitrogen purge, the lower without. The spectrometer does not have a UV grating, and so the sensitivity falls off rapidly with deceasing wavelength. It is clear, however, that the flashlamp is producing significant light flux in the 185 nm region.

This increased vacuum UV intensity has enabled us to obtain, for the first time, RELIEF images of vibrationally excited oxygen using the Raman cell to tag, and the flashlamp to interrogate. A typical pair of images is illustrated in Fig. 8. The flashlamp optical set-up is similar to that of Fig. 5, except that the 50 mm focusing lens was positioned as close as possible to the inner wall of the purgable enclosure. (The air path between the lens and the focus was not purged.) The focal volume of the flashlamp

output was approximately cylindrical, 3mm in diameter by 1-2 cm long. The tagging beams from the Raman cell were focused with a 300 mm lens, and intersected the flashlamp interrogation volume at a slight (~5°) angle. The resulting images were captured at 90° with respect to the tagging beams using a UV-intensified CID camera and a Corning 7910 glass filter. It was found that this filter, while decreasing the signal, increased the contrast between the tagged line and the background.

The images in Fig. 8 appear fuzzy due to the relatively long exposure time from the flashlamp. There is also significant background from O_2 Schumann-Runge fluorescence, which has a large cross section in the 180-185 nm region. It is anticipated that further work will allow us to significantly improve upon the quality of these images.

SUMMARY AND FUTURE WORK

The Raman cell has been developed and characterized to the point where it is now the method-of-choice for O_2 flow tagging. It is routinely used in two of our laboratories, and a cell has been constructed and operated at NASA-Langley Research Center. The output of the UV flashlamp has been increased by more than a factor of ten, and the first RELIEF images of vibrationally tagged oxygen have been obtained.

Future work, contingent upon continued support, will focus on collaboration between Princeton and NASA-Langley in performing flow tagging measurements in NASA LARC facilities. Further development of the UV flashlamp, with the goal of improved sensitivity, contrast, and timing, is also anticipated.

REFERENCES

1. R.B. Miles, J.J. Connors, E.C. Markovitz, P.J. Howard, and G.J. Roth, Exp. in Fluids 8, p. 17-24 (1989).

2. W.R. Lempert, B. Zhang, R.B. Miles, and J.P. Looney, J. Opt. Soc. Am B 7, p. 715-721 (1990).

3. M.B. Long, P.S. Levin, and D.C. Fourguette, Opt. Lett 10, p. 267-269 (1985).

4. J.F. Holzrichter and J.L. Emmett, Appl. Opt. 8, p. 1459 (1969).

5. R.B. Miles and W.R. Lempert, Final Technical Report for NASA-LARC, Grant #NAG-1-1011, June 20, 1990.

TABLE I

SUMMARY OF CELLS INVESTIGATED

	Cell	f_L	Pulse Duration	Gas Mix (O_2:He)	%1st Stokes	Emax
1.	2 m	2 m	10 nsec	450:0	3-4%	50 mJ
2.	2 m	1-2 m	10	450:550	4-9%	>250 mJ
3.	2 m	1 m	5	450:550	8%	>250 mJ
4.	2 m (2 passes)			400:600	~17%	>220 mJ
5.	6 m	4 m	10	200:400	11-12%	>250 mJ
6.	1 m *(Cylindrical Multipass - 9 passes - Limited to 1Hz)*					
			10	400:100	~30%	>250 mJ

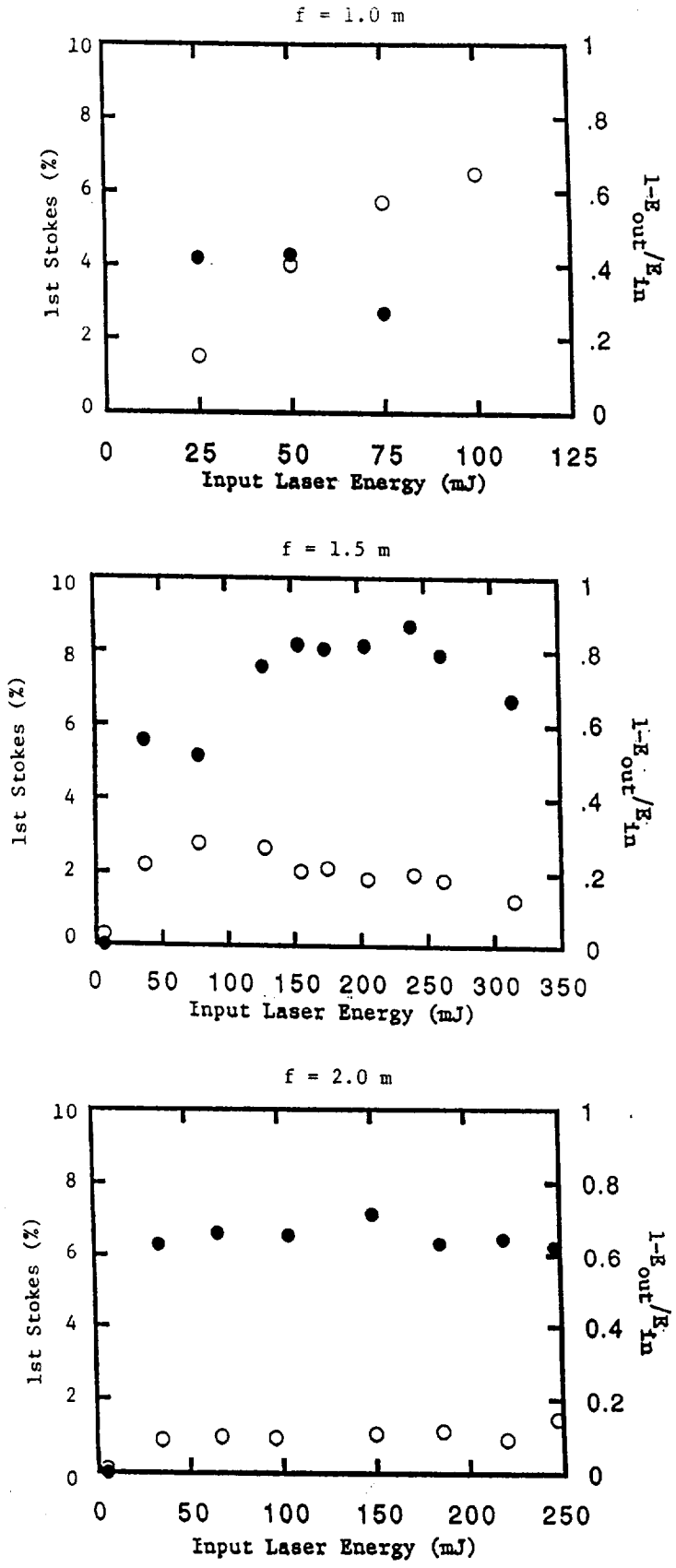

Figure 1. 1st Stokes Conversion Efficiency (o) and Fractional Loss (o) as a Function of Laser Pulse Energy for 1.0, 1.5, and 2.0 m Focusing Lens.

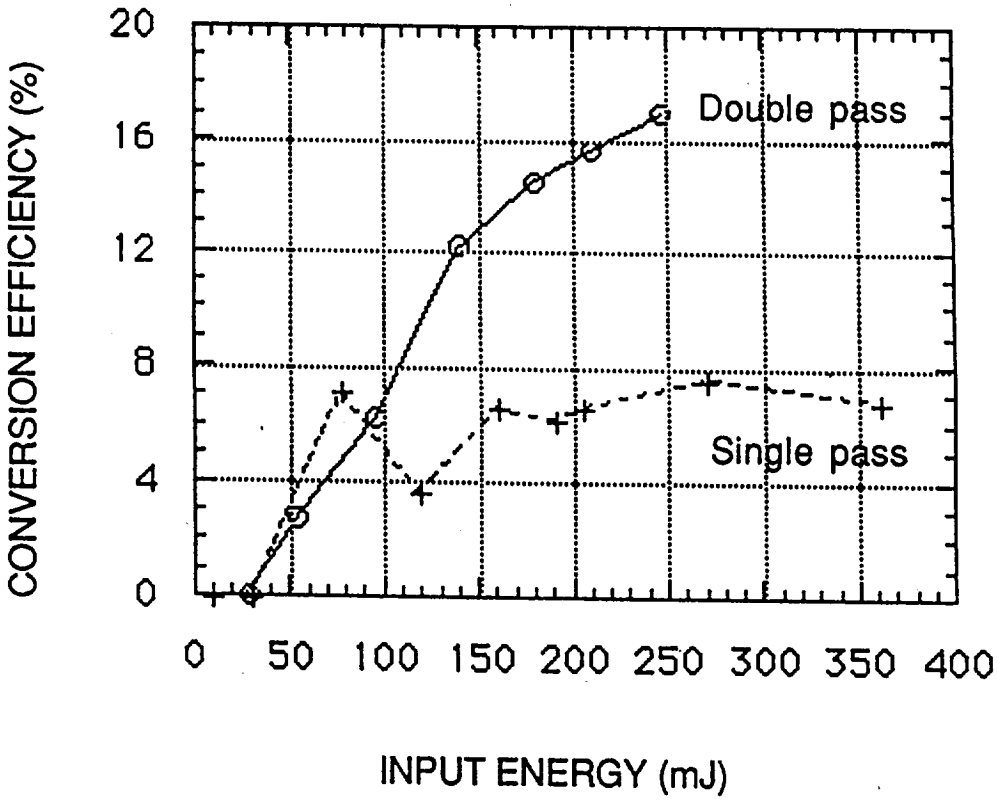

Figure 2. Single Pass (+) and Double Pass (o) 1st Stokes Conversion Efficiency for 5 nsec Pulse Duration Laser. The Cell Length is 2.0 m and Focusing Lens Focal Length is 1 m.

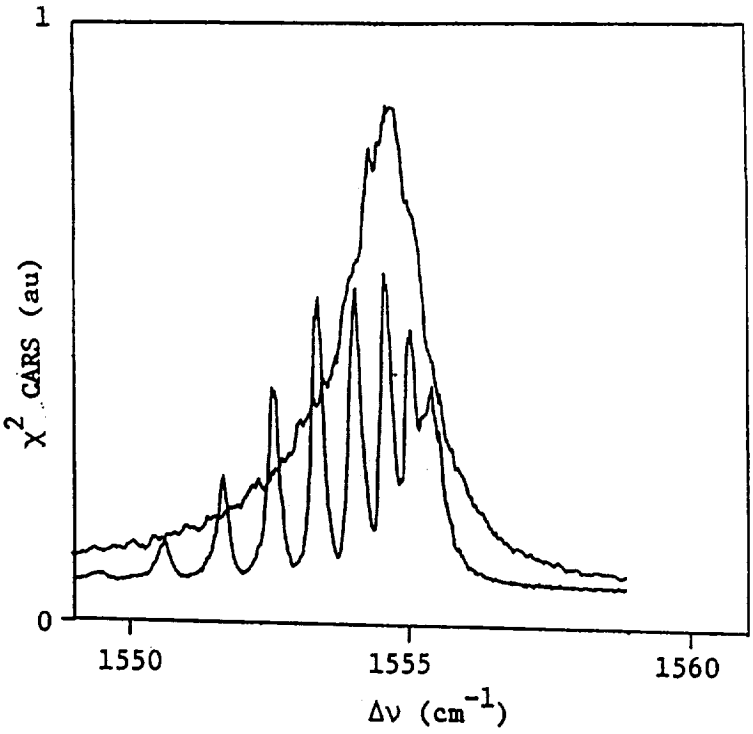

Figure 3a. Experimental CARS Spectra for Pure O_2 at 450 psi (Upper Trace), Along with Room Air Reference (Lower Trace).

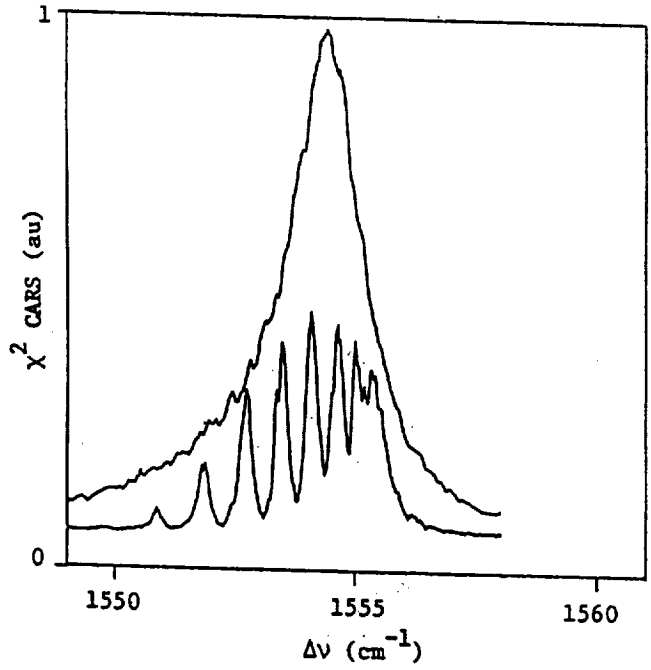

Figure 3b. Experimental CARS Spectra for Mixture of 450 psi O_2 and 550 psi He (Upper Trace), Along with Room Air Reference (Lower Trace).

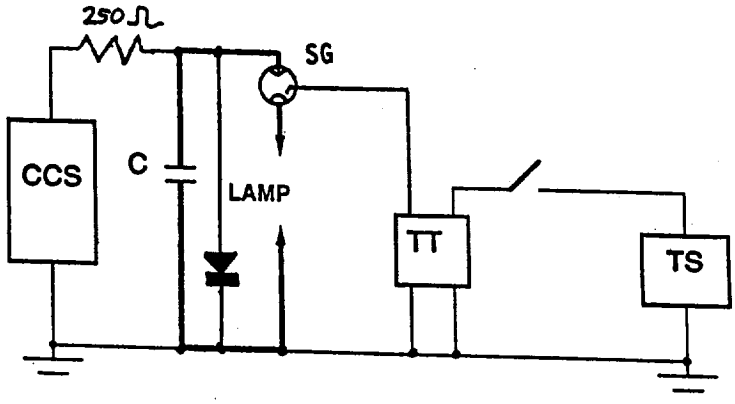

CCS = CAPACITOR CHARGING POWER SUPPLY
TT = TRIGGER TRANSFORMER
TS = TRIGGER POWER SUPPLY
C = CAPACITOR
SG = SPARK GAP

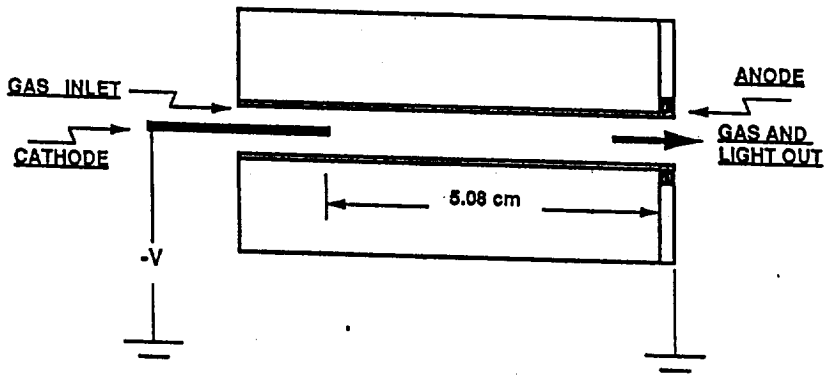

Figure 4. Schematic Diagram of Original Version of Coaxial UV Flashlamp. The Spark Gap has been Removed from the Current Version.

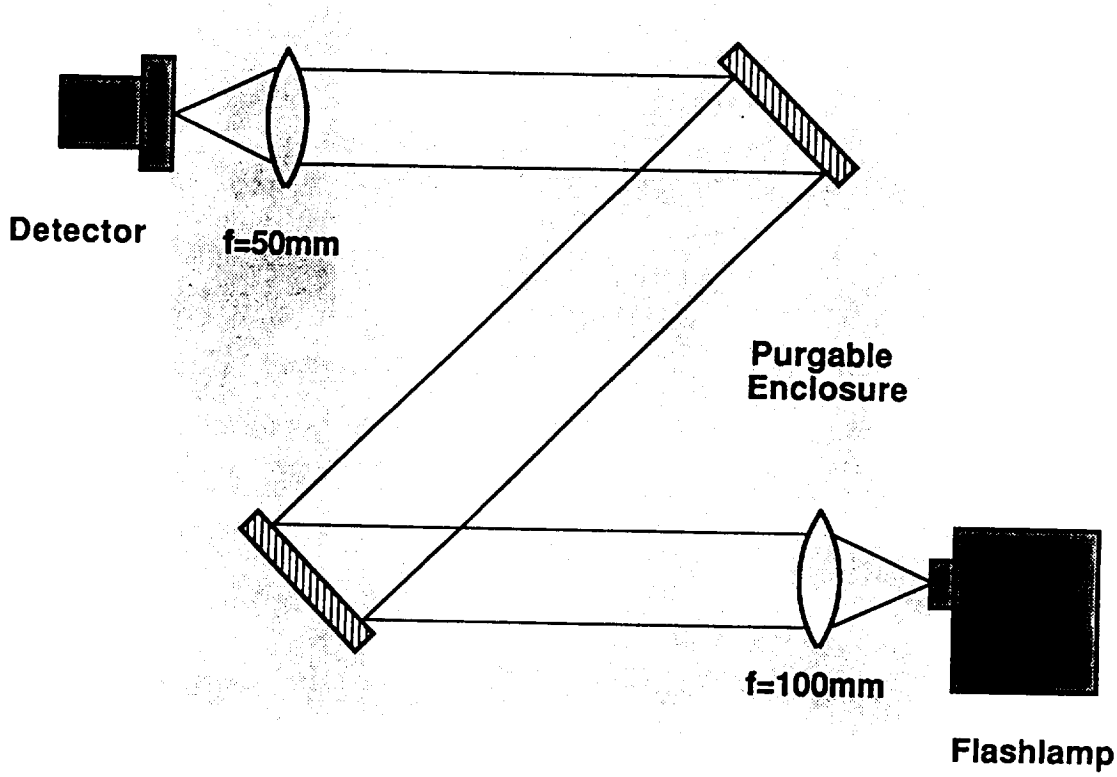

Figure 5. Schematic Diagram of Flashlamp Optical Filtering and UV Energy Measurement.

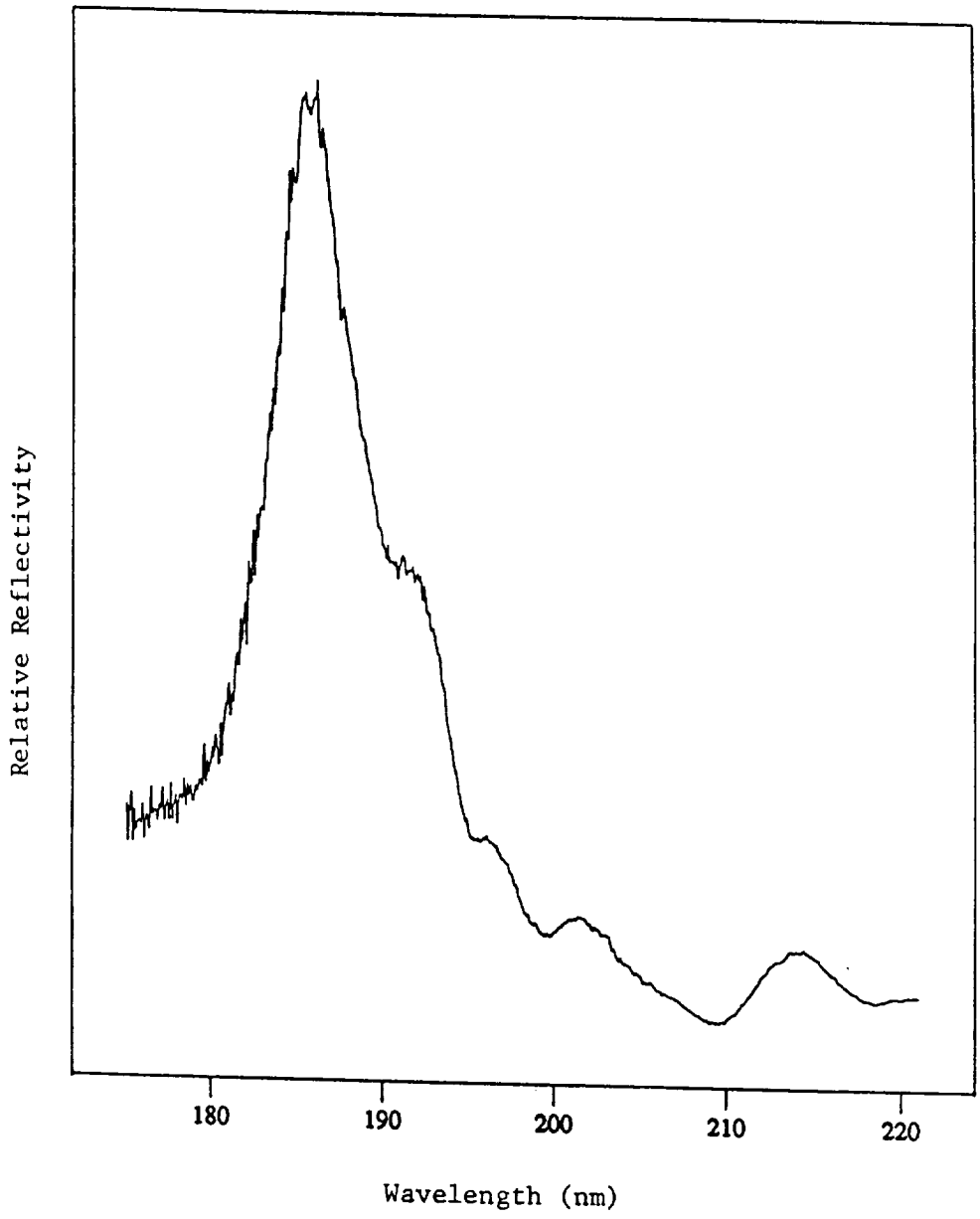

Figure 6. Relative Reflectivity of Mirror Pair as a Function of Wavelength.

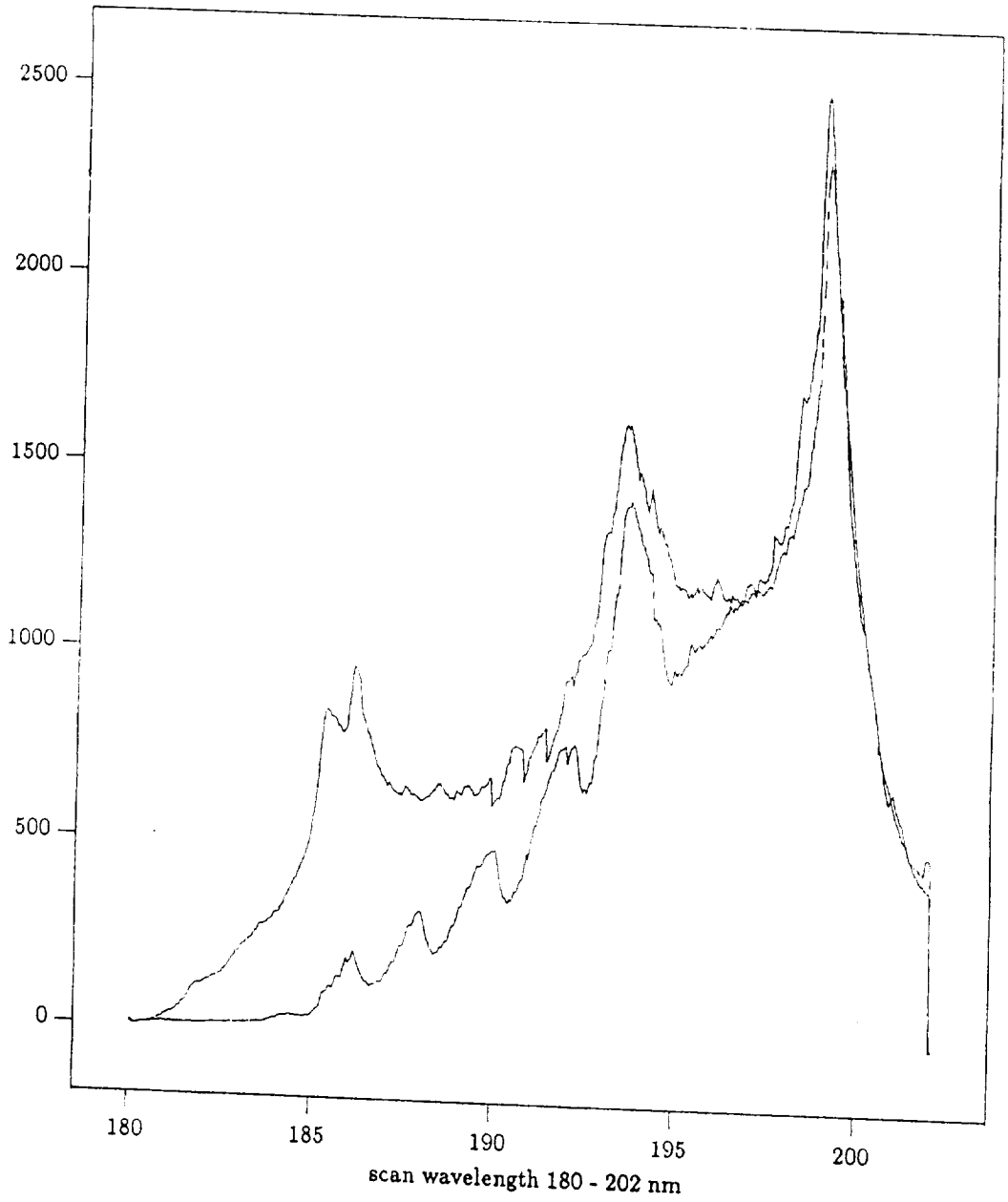

Figure 7. Experimental Lamp Output as Function of Wavelength With (Upper Trace) and Without (Lower Trace) N_2 Purge of Optical Path.

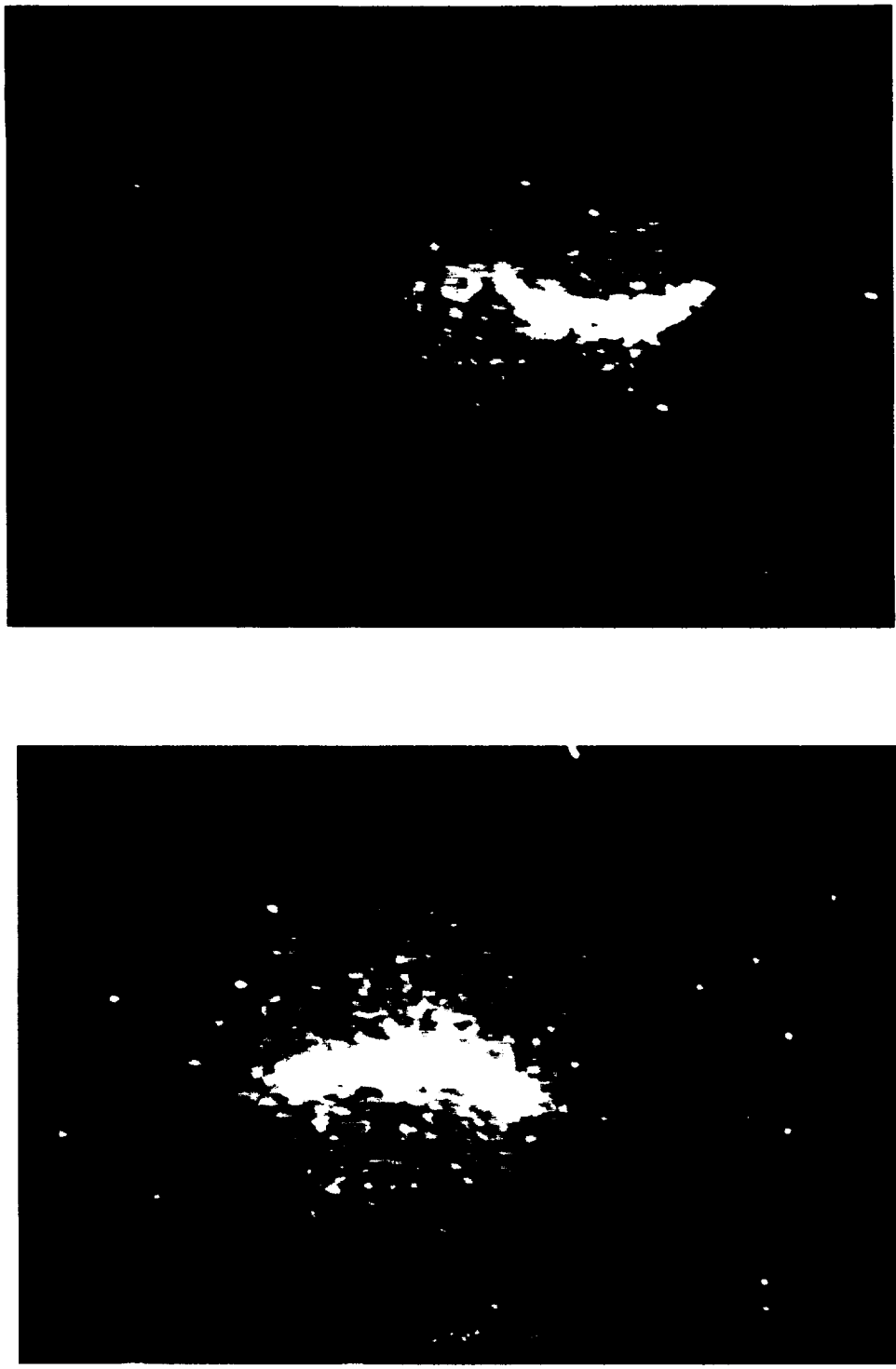

Figure 8. Selected Images of Displaced Lines Using Raman Cell for Tagging and UV Flashlamp for Interrogation.

REPORT FOR NASA-LANGLEY CONTRACT #NAG-1-1157

p. 40

B. "THE APPLICATION OF THE RELIEF TECHNIQUE FOR VELOCITY FIELD MEASUREMENTS IN THE ASTF C1 TEST CELL"

Attn: Dr. Ron Kohl
Sverdrup Corporaton
Buildings 1099, Room F203
M.S. 900
Arnold Air Force Base
Tennessee 37389-9998

1. INTRODUCTION

The ASTF C1 Test Cell is to be configured for propulsion tests of NASP engines over flight Mach number conditions ranging from 0.5 to 3.8. This facility is capable of continuously generating a 5' x 5' square free air jet flow field at a local Mach number up to 3.32 with a density of between 0.134 and 0.048 amagat and a static temperature of 257 K or less (see Table 1). It is the goal of this report to examine the potential of the RELIEF (Raman Excitation + Laser-Induced Electronic Fluorescence) velocity measurement technique for measuring the three-dimensional velocity profile across the exit plane of this jet and the entrance plane to the test engine under these conditions. Velocity measurements must be done to an accuracy of better than 1%. Flow direction must be measured to better than 1^{o} for inlet performance evaluation. Measurements to these specifications need to be done with a grid spacing of approximately 1/100th of the cross-sectional dimension of the free jet exit in a time not greater than 30 seconds.

The RELIEF velocity measurement method is based on vibrationally tagging oxygen molecules and observing their displacement after a short period of time (1). It requires a Nd:YAG laser for tagging the molecules, an argon-fluoride laser for interrogating the molecules after they have moved, and a camera system to image the displacement. A simplified diagram of the RELIEF set-up is shown in Fig. 1. The RELIEF technique has recently been used to

measure the velocity of a small Mach 2 pressure-matched free jet to approximately 0.5% accuracy. The technique has previously been applied in an underexpanded free jet air flow up to Mach 4. In that instance, however, the static temperature was approximately 60 K and the pressure was approximately 1 psi. The corresponding density, 0.288 amagat, was considerably greater than that expected in the ASTF C1 facility during Mach 3.8 operation. While this reduction of density is of concern, it should be noted that the higher temperature in the ASTF facility significantly enhances the interrogation signal intensity. Densities as low as 0.13 amagat at room temperature have been observed in stationery air. Reaching densities as low as 0.048 amagat is expected to be achievable, particularly in view of the large size of the lines to be marked, but further research is needed to verify that expectation.

In order to achieve the required number of velocity measurements within the 30 second time interval, multiple intersecting lines must be written into the wind tunnel facility. Multiple line marking has previously been accomplished in free jets, but this has been done by reflecting the tagging laser beams back through the test section. In the ASTF facility it is best to design a system that is single-ended, so that the mirrors on the other side of the flow field do not have to be included. Furthermore, the tagging lines should extend across the test section, if possible, so that dynamic refocussing of the optics is not required. Due to diffraction effects, this means that the diameter of the lines to be marked will be significantly larger than those previously marked in the small free jet. As a consequence, a tagging laser source capable of much higher peak power than the sources presently in use will be required. This suggests the use of a picosecond laser system rather than a nanosecond laser system for tagging. The increased size of the lines has the advantage of significantly enhancing the number of photons collected per resolvable element. By employing a picosecond laser source and by scaling up the light detection collectors as well as the interrogation laser source, multiple line grids can be marked into the ASTF C1 facility and interrogated for high accuracy, three-dimensional velocity field measurements.

This report outlines the specific details of such an apparatus. In some cases, such as for that of the picosecond laser source, the operating performance has not yet been determined. In other cases, such as for the interrogation system and the imaging camera, performance can be scaled from present laboratory results. Issues relating to optical access and the geometry of the ASTF flow facility are also addressed in this report. It is the goal of this effort to design a RELIEF-type system which fits within the geometrical constraints of the actual test configuration for the NASP engines.

A complimentary study is underway at Princeton University in the Applied Physics Laboratory to measure the vibrational relaxation dynamics of oxygen in the presence of other molecular species which are characteristic of the air in the ASTF C1 facility. The principle goal of this study is to assure that oxygen is vibrationally relaxed as it exits from the nozzle so that there is not a significant amount of background scattering from vibrationally excited oxygen molecules which might otherwise obscure the RELIEF signal. RELIEF measurements have, to date, been made up to 700 K (2). But it is clear that a significant vibrational nonequilibrium will cause a degradation in the signal level and may limit the RELIEF diagnostic performance. While it is highly unlikely that a significant vibrational nonequilibrium exists in the nozzle exit of the ASTF C1 facility, the complimentary study will assure that this is the case and will also delimit other environments in which the RELIEF diagnostic method might be applied.

2. FLOW TAGGING

Figure 2 shows an energy level diagram of the RELIEF process. The up and down arrows on the left indicate the tagging step in which two high-intensity lasers, separated in frequency by the vibrational frequency of oxygen, drive the molecules into their first vibrationally excited state. Since this step is a nonlinear process, these two lasers must be focussed to high enough intensity (watts/cm^2) to drive a significant fraction of the molecules into the vibrationally excited state. The third arrow corresponds to the ArF laser which drives the excited molecules to an upper electronic

state after they have moved. This step is a linear process, so the ArF laser must have an energy fluence (joules/cm^2) high enough to further excite as many of the tagged molecules as possible. While most of the molecules dissociate, some return to the lower electronic manifold and radiate light (wavy arrows) which is imaged by the camera.

In the initial experiments, the apparatus consisted of a frequency doubled Nd:YAG laser (532 nm) and a frequency tunable dye laser (580 nm). Part of the Nd:YAG laser beam was used to pump the dye so that both lasers were synchronized in time. This configuration required that the dye laser beam be overlapped spatially with the frequency doubled Nd:YAG laser beam, that the dye laser be properly tuned so that the frequency difference corresponded to the vibrational frequency of oxygen, and that proper delays be incorporated so that the two pulses arrived at the sample volume at the same time. More recently, a much simplified system has been designed (shown in Fig. 1) which uses a high-pressure stimulated Raman cell to generate the second beam required for tagging (3). In the most recent configuration, a high-intensity, frequency-doubled Nd:YAG laser beam is passed into a high pressure cell containing a mixture of helium and oxygen gas. Through frequency conversion by stimulated Raman gain, a portion of the energy of the frequency-doubled Nd:YAG laser is converted to a second laser beam which is lower in frequency by the vibrational frequency of the oxygen molecules in the cell. As a consequence, two beams exit the cell, the residual 532 nm frequency-doubled Nd:YAG laser light and a newly generated spatially overlapping 580 nm beam. By properly selecting the pressure in the high pressure stimulated Raman cell, the frequency difference between these two beams can be made to coincide with the vibrational frequency of oxygen in 1 atm or lower pressure air. As a consequence, the two beams can be refocussed into the test facility to mark lines by vibrationally exciting the oxygen molecules.

At present, work is underway to improve the conversion efficiency of the high pressure stimulated Raman cell to achieve the optimum intensity balance between the two beams. Ideally, both the residual 532 nm and the generated 580 nm beams have the same intensity to most efficiently mark the flow

field. The present cell configuration gives a maximum of approximately 15% conversion, which, with other losses, yields approximately a 5:1 intensity ratio between the residual doubled Nd:YAG laser and the newly generated beam. Attempts to improve the conversion efficiency are underway using multi-pass cells or laser dyes. Nevertheless, very good tagging has been accomplished using the present configuration. The major motivation to move towards the ideal intensity ratio is to avoid optical breakdown of the air and damage to windows. Another important aspect of the high pressure stimulated Raman gain method for generating the tagging laser beams is that the Nd:YAG laser can be operated at broad bandwidth and simultaneously generates a broad bandwidth of shifted light. This broad bandwidth allows simultaneous pumping of several oxygen rotational states for flow marking. Since the molecules are distributed in various rotational states by thermal mechanisms, this means that a larger percentage of molecules is available for flow tagging and, consequently, stronger lines can be written.

In order to upgrade this tagging capability for the ASTF facility, a large increase in laser intensity is required. This arises from two causes: the first is that lines on the order of 1.5 meters in length need to be written with the laser system. As a consequence, the laser beams cannot be focused as tightly as in the small-scale facility heretofore used. The increase in the beam area must be compensated for by an increase in the power in order to maintain intensities at the level required for tagging. The second reason that higher powered lasers are required is that numerous lines must be written into the flow field simultaneously in order to generate grid-type patterns for multiple velocity measurements during a single pulse. Since the laser systems will have a maximum repetition rate of approximately 15 pulses/second, and only 30 seconds is available for the measurement time, a minimum of 23 velocity measurements must be made with each pulse in order to achieve the 10^4 velocity elements desired.

a. <u>Saturated Tagging</u>

In order to achieve the highest tagging efficiency possible, the oxygen molecules must be driven into saturation by the tagging laser pulses. The concept of saturation implies that the population has reached an equilibrium

where the pumping rate out of the ground state and into the excited state is just equal to the collisional energy transfer rate into the ground state and out of the excited state. In the case of oxygen, the collisional processes are most likely rotational energy transfer collisions for both vibrationally excited and unexcited molecules. In oxygen at 1 atm pressure, the intensity product of the green (532 nm) and the orange (580 nm) corresponding to saturation, K, has been measured to be approximately 4.2×10^{21} W^2/cm^4 (4). This measurement was made with a very narrow frequency 532 nm beam and a narrow linewidth tunable dye laser in the vicinity of 580 nm. The number is probably high for this configuration since the beam profiles of the two lasers were not identical, and, therefore, the overlap in the sample volume was imperfect. (The effect of the laser bandwidth, particularly as a function of the air density has also not been explored.) For lack of a better estimate, we will use the value of 4.2×10^{21} W^2/cm^4 for scaling.

The lasers used had 10 nsec pulse lengths, and one can assume that at saturation, the pumping rate just equalled the collisional rate:

$$W = I_G I_O A = 1/\tau \qquad (1)$$

Where W is the pumping rate in transitions per second per molecule, I_G is the intensity of the 532 nm laser (green), I_O is the intensity of the 580 nm laser (orange), A is a constant, and τ is the time between collisions. This expression must be scaled for different densities and different laser pulse lengths in order to determine optimum intensities. At 1 atm, pure oxygen has a time between collisions of approximately 6×10^{-11} seconds (3). So long as this time is short compared to the laser pulse length, the saturation model still applies. In the regime where the laser pulse length is shorter than the collision time, coherent phenomena occur and it may be possible to achieve very large populations in the vibrationally excited state by coherent excitation. Due to the different angular momentum quantum numbers associated with each transition, a calculation of that population would require sophisticated quantum mechanical modelling as well as full knowledge of the temporal and frequency characteristics of the pump. However, with shorter pulses, one can experimentally optimize the pumping by

observing signal intensity. With 10 nsec lasers, this coherent regime will occur with gas densities less than 0.006 amagat. By shortening the laser pulse length we can move into this regime at gas densities corresponding to those projected for the experiment. For example, a 100 picosecond laser would pump molecules in the collisionless regime for gas densities 0.6 or less of atmospheric. Such a laser also has 100 times higher power for the same pulse energy as a 10 nsec source. If the conversion efficiency of this type of laser in a high pressure stimulated Raman cell were to be the same as that of a 10 nsec laser source, we would achieve an intensity product 10,000 times higher for the same pulse energies.

It is this dramatic increase in the pumping which makes picosecond sources particularly attractive for the ASTF facility. A picosecond laser allows a reduction of the energy of the laser beam with a simultaneous increase in the power. The reduction in energy reduces the breakdown threshold, a problem both in the gas and at windows. The higher power leads to an increase in intensity which means that the laser need not be focused as tightly and, consequently, longer lines can be written. An additional benefit of a picosecond source is that competing mechanisms in the high pressure stimulated Raman cell, including backward Brillouin and backward Raman scattering are suppressed by the short pulse length. If the pulse is transform limited, i.e., the frequency bandwidth is just the Fourier transform of the pulse time profile, then the product of the pulse time (full width at half maximum) times the pulse bandwidth in Hz (full width at half maximum) equals 0.44. Thus, a 100 picosecond source has a minimum linewidth of 0.15 wavenumbers (4.4 GHz). In practice, the 100 picosecond commercially available Nd:YAG laser source (Continuum) is not transform limited and has a linewidth of approximately 1 wavenumber. This 1 wavenumber linewidth is capable of overlying the J=1,3,5, and 7 lines simultaneously for vibrationally tagging oxygen molecules. At 200 K, 53% of the oxygen molecules fall into one of these levels. Preliminary experiments using a picosecond laser source at the Princeton Plasma Physics Laboratory indicate that very high conversion efficiency in the high-pressure simulated Raman cell can be expected. Further research with the picosecond laser source, including the design of the high-pressure stimulated Raman cell and

efficiency of flow tagging, will be required to determine if these predictions are, in fact, true.

b. **Focusing**

Due to the refraction of light, there is a fundamental limit on the region over which a high intensity laser can be focussed. This is usually expressed as:

$$b = \frac{2\pi w_o^2}{\lambda} \qquad (2)$$

where b is the confocal beam parameter and it is the distance between the points where the intensity drops by a factor of 2, compared to the highest intensity point. w_o is the beam waist measured as the $1/e^2$ intensity radius of a Gaussian beam across the point of highest intensity. λ is the wavelength of the laser. By integrating across the focal point, an equivalent area associated with the peak intensity can be found. In other words, if the peak power of the laser is P, then the peak intensity, I, will just be P/A, where:

$$A = b\lambda/4 \qquad (3)$$

With the 10 nsec laser sources that are currently used, saturation intensity is achieved when $I = \sqrt{K} = 6.5 \times 10^{10}$ W/cm^2. If the laser energy is 100 mJ/pulse, it has a peak power of approximately 10^7 W, so to achieve strong tagging, the beam must be focussed to an area of 1.5×10^{-4} cm^2. This corresponds to a beam waist of approximately 100 microns, or, at 532 nm, a confocal parameter of 12 cm. This implies that the line marked will be on the order of 12 cm long. In order to increase that distance to 1.5 meters, the beam area must be increased by a factor of 12.5, or the beam waist by a factor of 3.5. Consequently, to maintain the same intensity, the power of the lasers must be increased by a factor of 12.5. Thus, a 1.25 J beam would be necessary at both frequencies, requiring a Nd:YAG laser with an output in excess of 3 J. Clearly, such a laser would be very difficult to build and might require that the last stage be a glass amplifier so that the repetition rate would be severely limited. The alternative approach,

therefore, is to move towards picosecond sources, where the power can be dramatically increased. For example, a 100 picosecond Nd:YAG laser source with an output energy of 100 mJ will have a peak power 100 times that of the 10 nsec source. This is well in excess of the factor of 12.5 required to mark a single 1.5 meter long line. The excess energy of such a source can therefore be used to simultaneously mark multiple lines so that many velocity components can be recorded with a single pulse.

The tagged line persists as long as the oxygen molecules remain vibrationally excited. In pure oxygen at 1 amagat this corresponds to 27 milliseconds (5). The vibrational lifetime of oxygen will, however, be substantially shorter in the presence of other molecular species. This is particularly true in the presence of water vapor which is a triatomic molecule with a vibrational energy level that is close to the vibrational energy of oxygen. Our preliminary measurements indicate that oxygen in the presence of saturated water vapor levels at 1 atm and room temperature corresponding to 0.02 mass fraction has a lifetime on the order of 2.0 μsecs (6). Other molecules that may possibly be strong quenchers include CO_2 and ozone. The quenching rate of oxygen by nitrogen is expected to be slow since nitrogen is a diatomic molecule whose energy levels are far from those of oxygen. Nitrogen itself has a very long vibrational relaxation lifetime since it, like oxygen, is a homonuclear diatomic molecule and cannot directly radiate energy. In the ASTF C1 facility, the air has a water vapor content of between 0.4 and 0.6 grains/pound mass. This corresponds to a mass fraction of 7.1×10^{-5} (7000 grains equal 1 pound mass). Scaling from 2 μsec, we can expect a vibrational lifetime of more than 500 μsec, or 1/2 meter of distance at 1000 m/sec. This estimate assumes a density of 1 amagat. At a density of 0.13 amagats, tagged lines should persist for several meters downstream. In high Mach number facilities which are visciated (heated by combusting a portion of the air), the water content in the flow stream is high, so the vibrational lifetime of the oxygen is substantially less.

For high accuracy velocity measurements, the time between tagging and interrogation needs to be long enough so that the displacement downstream is

large compared to the line diameter. For a flow field of 1,000 m/sec, a 10 μsec delay corresponds to 1 cm. For the accuracy needed for these measurements, a displacement of a few centimeters will be sufficient. Consequently, vibrational lifetimes on the order of several tens of microseconds will suffice. At present, measurements are underway at Princeton to establish more precisely the relaxation time of oxygen in the presence of other gas species. However, achieving delay times of this order are not expected to be a problem.

In addition to vibrational relaxation, the tagged line experiences some broadening due to thermal diffusion. The broadening expression is:

$$w' = (4\Delta t D + w_o^2)^{1/2} \qquad (4)$$

where w' is the Gaussian line radius, D is the molecular diffusion constant, and Δt is the time between tagging and interrogation. w_o is the beam radius of the line when it is written. At 1 atm, D = 0.21 cm^2/sec. From this expression it is clear that thermal diffusion becomes important when the diffusion scale is on the same order of magnitude as the linewidth. With the large linewidths expected to be written into the ASTF flow, thermal diffusion will be unimportant.

c. <u>Optical Breakdown</u>

At the high intensities required for flow tagging, optically induced breakdown becomes a potential problem. In the most serious case, the air itself can be broken down by the laser beams. More likely, however, will be the breakdown of dust particles or other contaminates in the flow field. A third concern is optical breakdown of window material, particularly when windows are placed close to the flow field region so the intensities of the tagging laser beams passing through the windows are high. A precise evaluation of the breakdown threshold is difficult since breakdown is a statistical event. Breakdown occurs due to the combined effect of multiphoton ionization and cascade ionization. Through multiphoton ionization, the laser produces a few electrons which are subsequently accelerated by the strong laser field and through collisions generate a

cascade which becomes a breakdown. In atmospheric pressure air, breakdown occurs in the vicinity of 50 GW/cm^2 with a 10 nsec laser at 532 nm. Note from the previous section that this is approximately the same as the saturation intensity for line tagging. As a consequence, for nanosecond lasers, the peak intensity must be reduced below saturation in order to avoid optical breakdown. It is important to note, however, that while the multiphoton ionization process is largely related to laser intensity, the cascade process requires time for the electrons to accelerate and collide with other atoms. Thus, optical breakdown is substantially less of a problem for picosecond sources. For example, in oxygen the breakdown threshold increases to 5 x 10^{13} W/cm^2 if a 25 picosecond source is used at 532 nm (7). In this regime, collisions do not occur during the pulse and the breakdown is largely due to multiphoton ionization. As the pressure increases beyond several atmospheres, cascade processes become important and the breakdown threshold decreases. At the low densities in the ASTF C1 flow facility, breakdown will be in the multiphoton limit if sources with pulse lengths on the order of 100 picoseconds or less are used. A similar reduction in breakdown problems with impurities and dust is expected, although a quantitative evaluation of that has not been done.

The breakdown threshold of window material is on the order of 20 GW/cm^2 and is a serious problem if the high intensity beams are to pass through windows close to the tagging region. Due to the very long confocal parameters required for long line marking, the beams will have high intensities for several meters outside of the flow field regime. For the experiments done to date, the windows have been placed many confocal beam parameters away, which has not been difficult since the marked lines and, consequently, the confocal beam parameters have only been a few centimeters in length. For the ASTF C1 facility, however, the confocal beam parameter will be on the order of 1.5 m, so windows will need to be located several meters from the test section. The use of picosecond lasers may alleviate this problem significantly since, once again, the breakdown threshold is significantly increased. For example, the breakdown threshold of quartz with a 100 picosecond laser is expected to be 10^{11} W/cm^2 which is somewhat above the saturation intensity for flow tagging. This, of course, assumes that the

windows are clean and, even so, the statistical nature of breakdown may lead to random breakdown events at significantly lower intensity levels. As a consequence, it is advisable to avoid passing the tagging beams through windows if at all possible.

3. INTERROGATION

The interrogation of the marked lines is accomplished using an injection-locked argon-fluoride laser whose frequency is tuned to overlap a transition from the V"=1 vibrational state of the ground electronic manifold to the V'=7 vibrational state of the excited electronic manifold. Subsequently, fluorescence from the V'=7 state is recorded by a camera so the line positions can be imaged. The very rapid predissociation rate of the upper electronic state of oxygen assures that fluorescence only occurs during the time the interrogating laser source is on. Typically, the argon-fluoride laser pulse lasts 10 nsec, so the interrogation is effectively instantaneous. In order to capture the displaced line, the interrogation volume must be large enough to accommodate the uncertainty in the flow velocity. The maximum interrogation volume is determined by the energy of the laser and the saturation fluence of the transition. (Fluence is defined as the energy/cm^2.) The saturation fluence of a transition corresponds to enough photons per unit area to excite all of the molecules within the volume. Consequently, the fluorescence signal level does not increase at fluences greater than the saturation fluence, so this determines the optimum focusing area for a particular interrogation source.

For vibrationally excited oxygen, the interrogation transition has a saturation fluence of 150 mJ/cm^2. If we assume we have a 100 mJ argon-fluoride laser, then the beam can be focussed to a total area of 0.67 cm^2 or less in order to produce the maximum interrogation signal strength. If the beam is focussed to this fluence and passed through the flow field, any marked lines falling within the illuminated volume will be interrogated. Since the flow has a predominate velocity vector, the interrogation beam may be shaped into a rectangle so that it forms a thick "slab" as it passes through the flow field. The orientation of this slab is then optimized to capture the displaced lines. The normal output of the argon-fluoride laser

(Lambda Physik LPX 301) is a rectangular beam on the order of 3 cm x 1 cm. If this laser can be operated injection-locked with a 1.2 joule output, this beam can be expanded and passed through the flow field to give a 4.9 cm x 1.6 cm slab extending all the way across the jet exit. This volume will capture a line displaced up to 4.9 cm with $\pm$ 9 degrees directional uncertainty. Of course, the sample volume can be moved farther downstream or reshaped to permit even greater displacements, but the direction of the velocity vector must be known to increasingly better accuracy. For initial measurements, it is wise to have the interrogation volume include the original tagged lines so the motion of the flow can be tracked from zero delay. Directional uncertainty in the plane of the interrogation slab does not create a problem since the lines are not convected out of the interrogation volume.

An area of concern is the ability of the interrogation laser to penetrate through the high temperature boundary layer and into the flow field. Whereas cold oxygen does not significantly affect the interrogation capability of the argon-fluoride laser, hot oxygen does. The presence of vibrationally hot oxygen in the boundary layer region will cause some portion of the argon-fluoride laser light to be absorbed before it reaches the high-speed region. That increased absorption level can be seen from Figs. 3 and 4. Figure 3 shows the molecular oxygen absorption in air at 1 atm and 300 K. Flow field interrogation is done on the P(19) and R(21) line transitions in the vicinity of 193.07 nm, as indicated in Fig. 3. Note that atmospheric pressure room temperature air has a small amount of absorption (0.003 cm^{-1}) at this wavelength from a small amount of vibrationally excited molecules naturally occurring in the atmosphere. This indicates that the intensity will be reduced by e^{-1} after 3.33 meters. Figure 4 shows the absorption profile of oxygen in air at 0.13 amagat at a temperature of 750 K. These conditions are similar to what is expected in the boundary layer of the Mach 3.8 ASTF C1 facility. Note that the absorption at 193.07 microns is increased to approximately 0.018 cm^{-1}. This is because, although the density of the air is significantly less, the temperature is higher, so a larger proportion of the molecules are in the first vibrational state and a larger proportion of those are in the J = 19 and 21 rotational energy

states. This factor of 6 increase in the absorption will cause some attenuation of the argon-fluoride laser beam as it penetrates into the flow facility across the boundary layer. For example, if the boundary layer is 10 cm thick, 16% of the laser light will be lost passing through it. This loss is equivalent to that seen in a 60 cm path length through room air. We note here that this suggests that, not only should the distance through the boundary layer be kept to a minimum, but the path of the laser beam passing into the flow facility will need to be purged with nitrogen or evacuated in order to minimize light loss. We should also point out that if the ArF laser can be frequency shifted with a deuterium Raman shifter, the fluorescence intensity can be increased by a factor of approximately 100, even taking into account only a few percent conversion efficiency. Work on this has been done by researchers at SRI (8).

4. CAMERA SYSTEM

The camera system must collect and image the laser-induced electronic fluorescence from the tagged lines at the time of interrogation. Since signal levels are critical, it is important to build a camera system which is capable of collecting as much light as possible. This leads to a large aperture camera system placed close to the flow field. In order to simultaneously resolve all three components of the velocity vector, two such cameras are required to provide stereoscopic images. In general, the camera system consists of a large diameter, low f number collection lens which forms an image on a double-intensified microchannel plate intensifier which is then coupled by optical fibers to a high resolution television camera. The development of the lens and camera system will be an important part of the ASTF project. Several important considerations need to be kept in mind. The first is that large aperture collection optics have an intrinsically small depth-of-field. This means that the observation plane is well defined and sources outside of that observation plane become rapidly defocused. In some cases, this defocusing might be used to determine out-of-plane velocity components. The major impact, however, is to limit the interrogation volume of the camera system. It is important, therefore, that the interrogation volume of the camera be carefully matched to the argon-fluoride laser illumination volume to optimize the system. A second consideration is the

rather narrow field-of-view which these cameras can observe. Approximately 15^{o} is typical. In order to get high collection efficiency, and low chromatic aberration, a reflector-type lens system is the most promising candidate. The difficulty is that low f number collection optics typically have significant off-axis distortion (coma). Coma can be corrected for specific object plane distances by incorporating an optical element at the entrance aperture to the camera. Alternatively, there are some configurations which can be built which have no coma. Advanced concepts in lens design have been proposed by La-Vision and Nye Optical Corporation, among others.

As an example, we choose the standard Nye Optical high-speed 150 mm focal length f/1.4 lens. If the observed line segment is 2 meters from the lens, the image plane will be 162 mm from the lens. This ratio leads to a demagnification factor, M = 12.3. The angular field-of-view of this camera is 16.5^{o}, corresponding to 58 cm. With the demagnification, this leads to an image plane width of 47 mm. Such a camera system would capture 2.24×10^{-3} steradians of the scattered light, or approximately a factor of 5 smaller solid angle than in the small-scale experiments done to date. This factor of 5 would be more than compensated for by the larger volume of tagged oxygen molecules. Nye Optical also believes they could build a 300 mm f/.9 UV lens system that would be capable of capturing 9 times the light level. This optical system is expected to have a collection angle of greater than 12^{o}, leading to a 42 cm field-of-view at 2 meters. Such a lens would have a demagnification of approximately 5.7, so the 42 cm would be projected onto a 73 mm image plane. Standard size microchannel plate intensifiers are 18, 25, 40 and 75 mm in diameter (ITT). In order to capture this field-of-view, a 75 mm intensifier would be needed. From the 75 mm image intensifier, optical fiber bundles may be used to transfer the image onto CCD or CID video cameras. In order to preserve the high resolution, it will be necessary to break the image into several sections, each connected to a separate videocamera. For example, a 2 x 2 or 3 x 3 array of sections may be connected to 4 or 9 video cameras so that high resolution can be maintained over a wide field-of-view. Since the important

portion of the field is a line which only moves a short distance, breaking the image into 2 or 3 segments along the line might be preferable.

In both collection lens arrangements the field-of-view is significantly less than the distance across the test section (5 feet or 1.5 meters). One potential way of significantly increasing the field-of-view in one dimension is to rotate the image plane so that a slanted planar field-of-view is imaged. It is interesting to note that the tangent of the slant angle of the observed field varies as M (the demagnification) times the tangent of the slant angle of the image plane. A diagram of this relationship is shown in Fig. 5 (9). This sort of imaging is often done with a bellows-type camera. By slanting the image plane 26°, a system with a magnification of 5.7 will observe an object plane slanted at 70°. The 150 mm lens will give the same angle with only a 13° rotation. Given the same field-of-view of the camera system, this will increase the observation plane extent by a factor of 3, which is approximately what is needed to extend the collection system to simultaneously observe all the way across the flow field. There will, of course, be some image distortion which will have to be accounted for with the image processing software. By using two such camera systems, each placed at a 20° angle on either side of the interrogation light sheet, stereoscopic images of a full cross-sectional portion of the flow field can be simultaneously imaged.

The resolution of the system will be determined by the microchannel plate intensifier pore size, the connecting optics, and the number of CCD or CID pixels in the videocamera system. The 75 mm ITT double microchannel plate intensifier has approximately a 100 micron point spread function. This means that there are approximately 750 channels across the intensifier face. By using tapered fibers or secondary imaging optics, the output of this intensifier could be imaged onto standard 11 mm CCD or CID videocamera arrays. Typical arrays have between 450 and 500 lines horizontal, and 484 lines vertical. Thus, a single camera observing the full 75 mm field will have a resolution limit of approximately 160 microns, whereas a multicamera system will have a resolution limit determined by the microchannel intensifier resolution. With the demagnification factor of the optical

collection system, a 100 micron resolution corresponds to 570 microns at 2 meters. This is the same order as the width of the line to be written. If one makes the assumption that the center of the line cannot be determined to better than 1 resolvable element (a conservative assumption since the line can usually be fit with better accuracy), then a 1% velocity measurement will require that the line move 100 times the 570 micron minimum resolvable distance, or 5.7 cm. If a slanted object plane is used, then somewhat greater displacement may be required in order to accurately measure the velocity at the most distant point. The closer points will be observed with greater resolution.

In order to achieve simultaneous images of multiple velocity components, a tagging configuration similar to that shown in Fig. 6 can be adopted. As mentioned earlier, in order to achieve 10,000 velocity measurements in 30 seconds, at least 23 points must be interrogated with each laser pulse. This can be done by intersecting 14 laser beams as shown in the figure. Two beams are focused such that they write a pair of lines separated by 1 cm all the way across the flow field. The other 12 beams can be somewhat lower power and more tightly focused so that they intersect these two beams at regular intervals. The purpose of these 12 beams is to introduce small crosses or "tic" marks on the two primary beams so that specific locations can be tracked. Due to the fact that each of the secondary beams only needs to mark a line which is on the order of 2 cm long, the beam power is less since the focussing area is small. The plane of this marked array lies in the flow direction and the interrogation laser illuminates the same plane. Thus, both lines with all their tic marks can be simultaneously interrogated as they move downstream. The cameras can be placed at 20^{o} angles above and below this plane in order to observe the displaced lines. While only 24 points across the flow field are observed at a single shot, the lines are continuous, so the velocity profile between the points will be observed. If needed, the 12 beams can be scanned together over approximately 10 cm to yield a higher resolution measurement along the principal lines. This would not require refocusing of these beams. In order to interrogate the entire flow field, the plane must be swept or traversed across the flow region of interest. Since the two principal lines, the tagging lasers, and the

cameras maintain a constant relationship with one another, all the hardware can be mounted on a platform which is then rotated or translated to sweep or traverse the interrogation plane across the flow field.

5. OPTICAL ACCESS AND GEOMETRY

The ASTF C1 facility produces a 5′ by 5′ free jet which will be used to test the NASP engines. A sketch of the expected configuration is shown in Fig. 7. The NASP engine will be mounted horizontally with its top in contact with the top lip of the jet exit. The jet will be directed downward at a 7^{o} angle to simulate the underside of the NASP vehicle. The width of the NASP engine is expected to be approximately 4′, and the bottom of the engine extends only 3′ down, leaving a portion of the jet passing below the engine to simulate flight conditions. The bottom of the engine is downstream of the top corresponding to a swept back entrance angle of 47^{o}. In order to avoid shock structures or expansion fans from entering the engine, shrouds are being placed both at the sides and a lip is being added to the bottom of the jet exit as indicated in Fig. 7. These shrouds and lip severely limit the optical access of both the jet exit plane and the engine entrance. The most reasonable optical access occurs from below the jet facility. However, this may be substantially obscured if a full 5′ lip is added onto the jet. If this is the case, then there is only a small gap below the engine and above the lip, through which to pass the diagnostics. Diagnostic beams passed through this gap may be severely distorted by the bypass air and the associated free shear layer. Alternatively, quartz windows could be installed in the lip in order to pass diagnostic beams into the test region. It is important to pass through as little of the boundary layer or turbulent by-pass flow as possible in order to avoid beam steering of the tagging beams, distortion of the image, and absorption of the interrogation laser.

Figure 8 shows a cross-sectional view of the nozzle exit with the flow tagging system diagrammatically shown, including the cameras at 20^{o} angles to the marking plane. The NASP engine entry is shown in the dotted line. This apparatus should fit within the 12′ diffuser, but will clearly have to penetrate any smaller diffuser section that might be added. If the laser beams and detection optics must observe the test section through windows,

there will be some loss, primarily due to window reflection and dirt which might accumulate. In addition, the windows will have to be large in order to provide for large size collection optics apertures and for sweeping or traversing the flow field. Structurally, the addition of windows is not expected to be a problem. Fused silica has very good thermal properties and its tensile strength actually increases at higher temperatures (see Table II). Quartz is, after all, a ceramic material and its properties are not unlike those of pyrex. The thickness of the quartz will have to be determined given the dynamic pressures of the flow field environment, but a 1/4" thick, 6 " by 6" grounded polished plate of Suprasil 2 costs on the order of $500. Larger plates will, of course, be needed and they will have to be especially fabricated. The transmission of a 10 mm thick Suprasil 2 window is approximately 90% at 193 nm. That transmission increases to about 93% in the visible region of the spectrum.

A potential problem with windows is the burn damage threshold associated with high-intensity tagging laser beams passing through them. As we previously discussed, for picosecond laser sources, this may be somewhat less of a problem than with the nanosecond sources that are used today. Nevertheless, the long confocal beam parameters required in order to get long lines marked through the flow field imply very high intensities close to the marked region. Since the window is at the boundary of the flow,there is no way of avoiding very high intensities passing through it. The other end of the laser beams can potentially hit the wall of the tunnel and generate significant scattering. However, this should not be a serious problem since marked lines are observed many microseconds later, and the detection system is collecting light in a different region of the spectrum.

The most desirable arrangement would be to have significant optical access underneath the jet exit plane and looking up into the engine entrance. For this reason, any reduction in the length of the bottom lip on the exit jet would have a substantial benefit. Our understanding is that the ratio of the test cell pressure to the static pressure of the jet will be kept at or below the Mach number. At a Mach number of 1.5, a pressure ratio of 1.5 leads to a shock angle of 53^{o}. (At Mach 3.4, a pressure ratio of 3.4 leads

to a shock angle of 31°.) If the lip is designed so the 53° oblique shock at Mach 1.5 does not enter the engine, it need only extend approximately 1.5 feet from the nozzle exit. This could open up an additional 3.5 feet for diagnostic access.

6. RECOMMENDATIONS

From this study it appears clear that there are no fundamental constraints which will prevent the RELIEF tagging technique from being implemented in the ASTF C1 facility. There are, however, a number of issues that must be addressed before such a system is configured. These include the following:

1. Tagging with a Picosecond Laser System. The RELIEF tagging apparatus will be greatly simplified if a picosecond laser system proves to be viable. It is expected that efficient tagging can be done with such a system using laser pulse energies on the order of hundreds of millijoules rather than pulse energies on the order of joules, or possibly tens of joules, which would be required otherwise. Furthermore, a picosecond source will substantially reduce problems associated with optical breakdown and window damage and may produce even more efficient tagging than is possible with nanosecond sources.

In order to take advantage of the potential offered by picosecond laser pulses, it will be necessary to construct a stimulated Raman cell with optimized conversion efficiency and to experimentally determine the resulting ability to tag flows under conditions similar to those anticipated in the ASTF C1 facility. Optimization of the Raman 1st Stokes conversion involves balancing the effects of several competing processes. This is accomplished by variation of oxygen pressure, oxygen/buffer gas ratio, cell length, and multi-pass resonator design. As mentioned previously, preliminary measurements performed in conjunction with the Princeton X-Ray Laser Facility, using 70 psec duration pulses, indicate that the Raman gain is high.

2. Low Density Operation. The ASTF C1 facility is expected to run at a density as low as 0.048 amagat. This density is a factor of approximately 6 lower than previous densities at which the flow tagging has been operated in supersonic free jets. In nonmoving atmospheric temperature air, lines have been observed down to 0.13 amagat, but signal levels were very low. With a combination of larger tagging volumes and higher tagging efficiency, it is expected that densities substantially lower than 0.048 amagat can be observed. However, this needs to be confirmed in laboratory experiments. One issue of concern is the role that collisional processes may play in both tagging and interrogation. For example, if many rotational reorientation collisions occur during either the tagging or interrogation step, then more efficient tagging and more efficient interrogation are possible. This may be occurring at high densities where the collision rate is fast enough during the 10 nsec tagging or interrogation time. At low densities, collisions will not be a factor and any enhancement due to this effect will be lost. If this effect is occurring, it means that the collected light is a nonlinear function of the pressure. Experiments to establish whether that is the case need to be done since that affects our scaling projection. The use of picosecond lasers with broad bandwidth to simultaneously pump many rotational states may alleviate this problem in the tagging step. In the interrogation step, however, one may find that a long pulse interrogation laser or an interrogation laser frequency shifted to the vicinity of 185 nm will give significantly higher signals.

3. Vibrational Relaxation Measurements. Measurements are currently underway to assure that there will not be a large percentage of vibrationally excited oxygen in the tagging region due to the high temperature in the plenum. These experiments will also identify the vibrational lifetime of oxygen molecules in the presence of water vapor and other species so that the maximum time between tagging and interrogation can be established once the constituents of the air are well known.

4. Development of the Lens and Camera Systems. The particular need to achieve high collection efficiency and good spatial resolution means that the lens collection system has to be well matched to the overall system

geometry. The possibility of using a slanted image plane to extend the field-of-view of the lens system needs to be examined and the practical collection and throughput efficiency of such lens need to be measured. The size of the collection lens will be determined by the signal levels at the low pressure limit. Since the cost of the camera system is strongly dependent on the lens size, experiments must be done to determine the smallest collection aperture necessary. The laboratory tests will be conducted using the 150 mm collection lens and a single camera system. The pre-facility test camera system will have to be designed based on the laboratory test results.

It is recommended that the following series of laboratory tests be conducted to address these issues:

A. Laboratory Tests

i. Optimization of flow tagging with picosecond pulses. The steps involved are as follows:
   a) Optimization of Raman cell conversion.
   b) Comparison with nanosecond flow tagging efficiency.
   c) Determination of optimum intensity for flow tagging as a function of density.
   d) Measurement of the gas, particle, and window breakdown thresholds with the tagging system.

ii. Determine the characteristics of lasers required to perform the interrogation step required for velocity measurements over the full operating range of ASTF C1 facility.
   a) Energy requirements for tagging of long lines and multiple crosses.
   b) ArF 193 nm interrogation fluence at operating conditions, particularly at low density.
   c) Investigation of the use of D_2 Raman cell for conversion of interrogation wavelength to 182.5 nm. Examine trade-off of higher fluorescence yield for lower laser fluence.

iii. Determination of camera/lens requirements.

a) Using results of (i) and (ii) above, determine lens collection efficiency requirements.

b) Using data from (iiia) above, and resolution requirements, design an optimized camera/lens system for capturing the maximum field-of-view.

iv. System integration and demonstration.

Upon completion of the tests of the three basic components, laboratory-scale instrumentation simulating the ASTF C1 system as closely as possible should be assembled. This system will be used to write and interrogate long lines including, perhaps, one or two crossing points using laser intensities and camera collection efficiencies comparable to that of a full-scale system. Line brightness, sufficient to perform accurate velocity measurements over the operating range of ASTF C1 should be verified. Velocity measurements at supersonic speeds for at least one or two crossing points could be done using a small laboratory flow facility.

B. Pre-Facility Tests

Following these laboratory tests, pre-facility tests need to be done with scaled up systems using a geometry which is identical to that to be installed in the C1 test cell. These pre-facility tests will require that a high energy picosecond source be used so that multiple lines can simultaneously be written to establish the viability of simultaneous multiple point interrogation. For these pre-laboratory tests, a high-power injection-locked argon-fluoride laser will be required. In addition, at least one, and preferably two, low f number, high-sensitivity camera systems need to be incorporated into the set up. Since the critical factor for the measurement is the temperature and density of the flow, many tests can be done using a temperature and pressure controlled test chamber to simulate the facility. As a practical matter, even the temperature control is not as important as is the density and gas mixture. At some point, however, it will be important to check what the effect of a high-temperature turbulent boundary layer will be on the operation of this device and establish what

the practical window damage limitations will be and other operating constraints.

Equipment Required for the Laboratory Tests

A. Equipment required for the test program:

1) 150 mJ, 100 picosecond Nd:Yag laser and upconversion optics. (Continuum Active/Active/Passive picosecond laser and doubling crystal and optics -- $125 K).
2) High pressure O_2 Raman shifter (built at Princeton -- $5K).
3) Lens and camera system (ITT 40 mm double microchannel plate intensified and fiber coupled camera -- $40 K, Nye Optical 150 mm f/1.4 collection lens -- $4.1K).
4) Low pressure test chamber (built at Princeton -- $10 K).
5) 150 mJ ArF injection-locked laser (Lambda Physik LPX 150 - $160 K).
6) D_2 Raman shifter for 185 nm tests (built at Princeton -- $15 K).

B. Added equipment for the pre-facility tests (size and cost depend on the outcome of the laboratory tests).

1) 400-800 mj, 100 picosecond Nd:YAG laser system.
2) Second lens and camera system.
3) 1 joule ArF interrogation laser (may or may not be injection-locked depending on D_2 Raman cell results).

Recommended vendors and more complete specifications for the above equipment can be found in Appendix A.

REFERENCES

1. R.B. Miles, J. J. Connors, E.C. Markovitz, P.J. Howard, and G.J. Roth, "Instantaneous Profiles and Turbulence Statistics of Supersonic Free Shear Layers by Raman Excitation + Laser-Induced Electronic Fluorescence (RELIEF) Velocity Tagging of Oxygen," Experiments in Fluids 8, p. 14 (1989).

2. G.S. Diskin, W.R. Lempert, and R.B. Miles, "Species and Velocity Visualization of Unseeded Heated Air and Combusting Hydrogen Jets Using Laser and Flashlamp Sources," AIAA 26th Joint Propulsion Conference, July 16-18, 1990, Orlando, Florida, AIAA Paper #90-1849.

3. W.R. Lempert, B. Zhang, R.B. Miles, and J.P. Looney, "Stimulated Raman Scattering and Coherent Anti-Stokes Raman Spectroscopy in High Pressure Oxygen," JOSA B 7, p. 715 (May 1990).

4. R.B. Miles, J.J. Connors, E.C. Markovitz, and G.J. Roth, "Coherent Anti-Stokes Raman Scattering (CARS) and Raman Pumping Lineshapes in High Fields," SPIE Vol 912: Pulsed Single Frequency Lasers; Technology and Applications, Ed. L. Rahn and W. Bischel, 1988, Paper #912-26, p. 184.

5. R. Frey, J. Lukasik, and J. Ducuing, Chem. Phys. Lett. 14, 514-517 (1972).

6. G. Roth, "The Determination of Molecular Oxygen's [Triplet Sigma Gerade Minus (v"=1) to Triplet Sigma Gerade Minus (v"=0)] Relaxation Rate in the Presence of Water Vapor," Senior Thesis Report, Department of Mechanical and Aerospace Engineering, May 4, 1989.

7. Y.E. E-D Gamal, "The Breakdown of Molecular Oxygen by Brief Pulses of Laser Radiation," J. of Physics D: Appl. Phys. 21, p. 1117-20 (1988).

8. G. Faris, M. Dyer, W. Bischel, D. Huestis, "VUV Stimulated Raman Scatatering of an ArF Laser in D_2 and HD," Paper CWF23, CLEO 1990, May 21-25, 1990, Anaheim, California.

9. L. Stroebel, View Camera Techniques, 5th Edition, Focal Press, Boston 1986.

TABLE I

SAMPLE NASP TEST CONDITIONS

STATIC CONDITIONS ON THE ENVELOPE
Gamma = 1.4

NO.*	USED?	FLT_MACH_NO	(10^3 ft) ALTITUDE	(atmo.) PRESSURE_AT_ALT	(K) TEMP._AT_ALT.	STAT_PRESS_RATIO	(atmo.) STATIC_PRESS.	(K) STAG. TEMP	LOCAL_MACH_NO	(K) STATIC TEMP	(m/s) VELOCITY	(Amagat**) DENSITY
1		0.5	0.0	1.000	288	1.00	1.000	302	0.50	288	170	0.968
1.9		0.5	0.0	1.000	288	1.19	1.190	302	0.00	302	0	1.074
2	NO	1.06	0.0	1.000	288	*	*	*		*	*	*
3	NO	1	17.4	0.512	254	*	*	*		*	*	*
4		1.5	29.9	0.298	229	1.42	0.423	332	1.25	253	398	0.456
5		2	38.6	0.198	217	1.47	0.291	391	1.75	242	546	0.328
6		2.5	45.4	0.143	217	1.57	0.225	488	2.21	247	696	0.248
7		2.77	51.3	0.108	217	1.63	0.176	550	2.45	250	777	0.193
8		3	54.8	0.094	217	1.69	0.159	608	2.65	252	845	0.172
9		3.5	58.5	0.077	217	1.19	0.091	749	3.08	258	993	0.097
10	NOT REAL	3.78	61.3	0.067	217	1.90	0.126	837	3.32	261	1076	0.132
11		3.78	61.3	0.067	217	1.90	0.126	822	3.32	257	1066	0.134
12	NO	0.24	0.0	1.000	288	*	*	*		*	*	*
13	NO	0.24	10.0	0.688	268	*	*	*		*	*	*
14	NO	0.97	10.0	0.688	268	*	*	*		*	*	*
15	NO	1	14.9	0.566	259	*	*	*		*	*	*
16		0.85	40.0	0.185	217	1.00	0.185	248	0.85	217	251	0.233
16.9		0.85	40.0	0.185	217	1.60	0.296	248	0.00	248	0	0.325
17	NO	1	40.0	0.185	217	*	*	*		*	*	*
18	NO	1.34	40.0	0.185	217	*	*	*		*	*	*
19		1.5	44.6	0.148	217	1.42	0.210	315	1.25	248	388	0.239
20		2	56.7	0.083	217	1.47	0.122	391	1.75	242	546	0.137
21		2.5	66.3	0.055	217	1.57	0.086	488	2.21	247	696	0.095
22		3	73.0	0.038	219	1.69	0.065	613	2.65	255	849	0.069
23		3.5	80.0	0.027	221	1.19	0.032	762	3.08	263	1002	0.034
24	NOT REAL	3.72	82.2	0.025	222	1.88	0.046	836	3.27	266	1070	0.047
25		3.72	82.2	0.025	222	1.88	0.046	822	3.27	262	1061	0.048

* Lower altitude limit is 1-11 (11 is 10 corrected for real gas in stag. temp. only).
Higher altitude limit is 12-25 (25 is 24 corrected for real gas in stag. temp. only).
(1 & 1.9 and 16 & 16.9 give the limits for these two [1 and 16] subsonic operation points -- stagnation conditions to free-stream (altitude) conditions)

** Amagat unit = density of air at STP (1 atmosphere, 273 K).

TABLE II

Tensile Strength - CFQ

	Tensile Strength (psi)		Poisson's Ratio	
20°C	7,100	7,200	0.170	0.170
300°C	9,600	8,700	0.175	0.172
450°C	10,200	9,100	0.180	0.179
600°C	10,700	9,500	0.184	0.188
750°C	11,000	10,100	0.187	0.194
900°C	11,800	10,800	0.190	0.200
1,000°C	12,200	---	0.192	---
SOURCE:	GE	CORNING	GE	CORNING

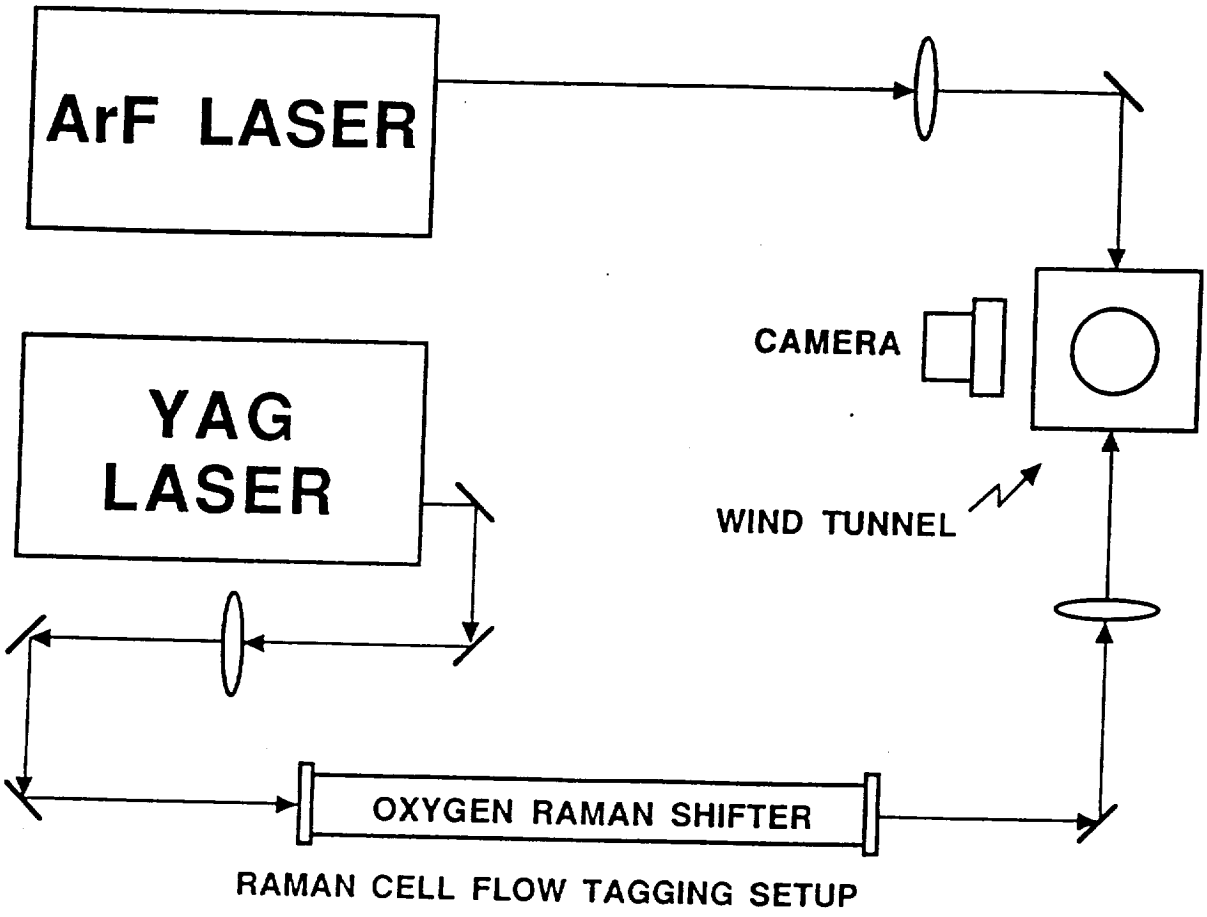

Figure 1. RELIEF flow tagging set-up with Nd:YAG laser for tagging, ArF laser for interrogation, and camera.

ENERGY LEVEL DIAGRAM FOR O_2

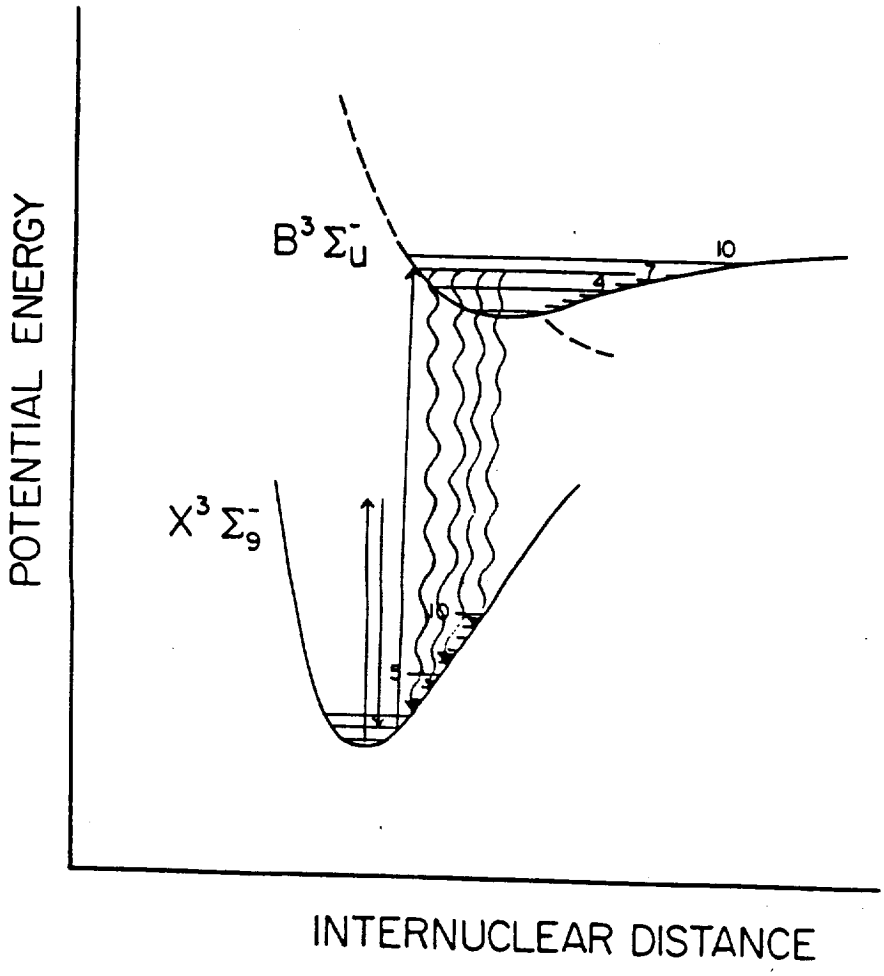

Figure 2. Energy levels of O_2 and the RELIEF process. The left pair of arrows indicate the tagging step. The third arrow indicates the interrogation step which leads to immediate fluorescence (wavy arrows). This fluorescence is imaged by the camera and shows the location of the displaced lines.

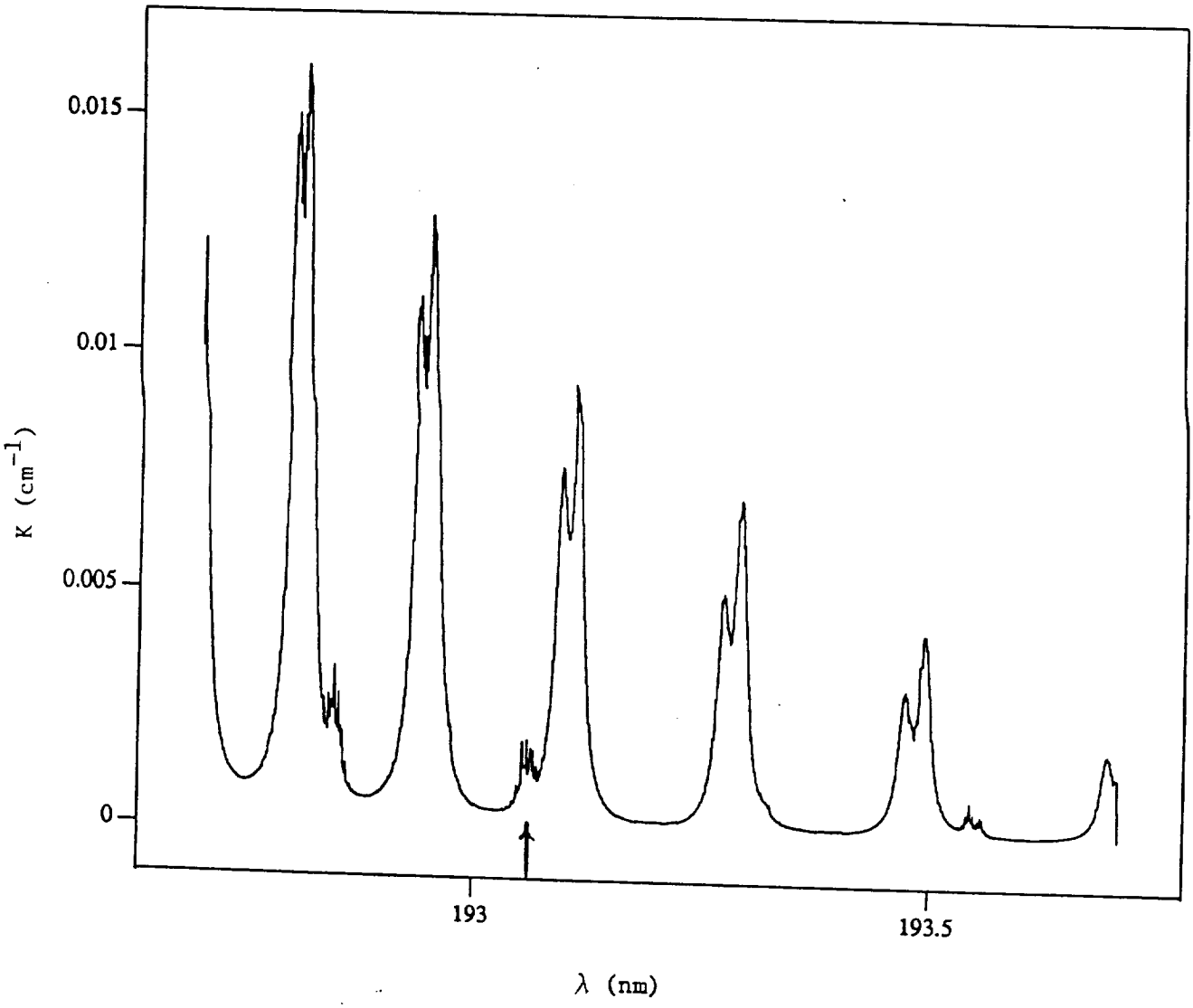

Figure 3. Absorption of atmospheric density air at 300 K. The frequency of the ArF interrogation laser is marked by the arrow.

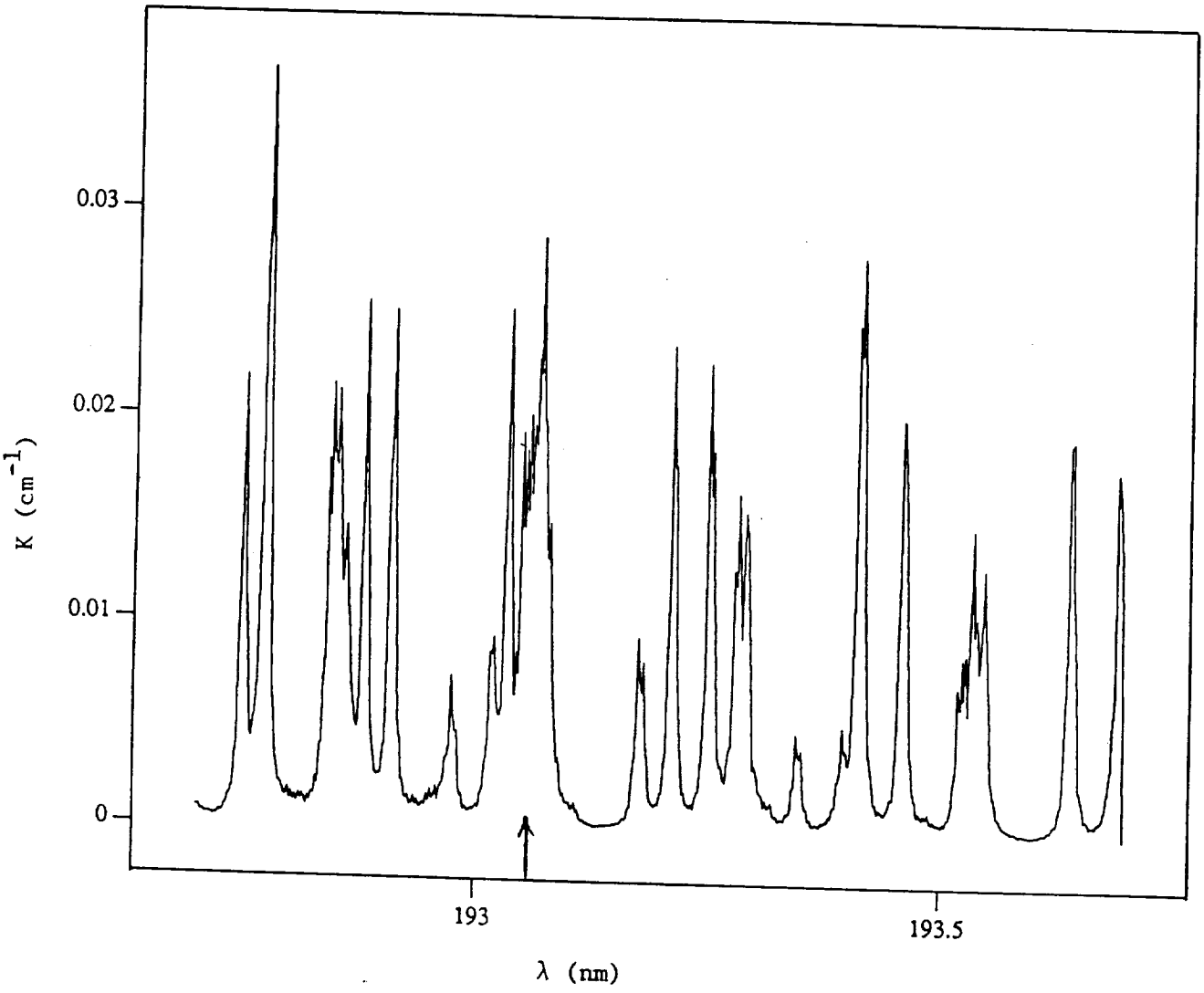

Figure 4. Absorption of 0.13 amagat air at 750 K, characteristic of the flow field boundary layer. The ArF laser frequency is marked by the arrow.

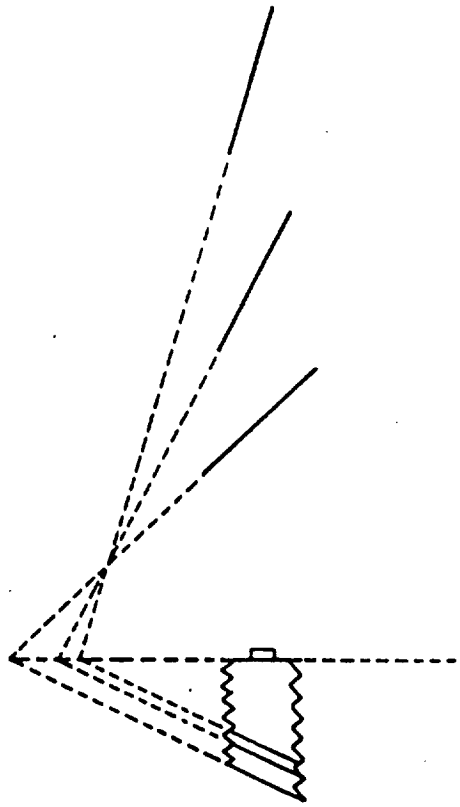

Figure 5. Relationship between object distance and the plane of sharp focus.

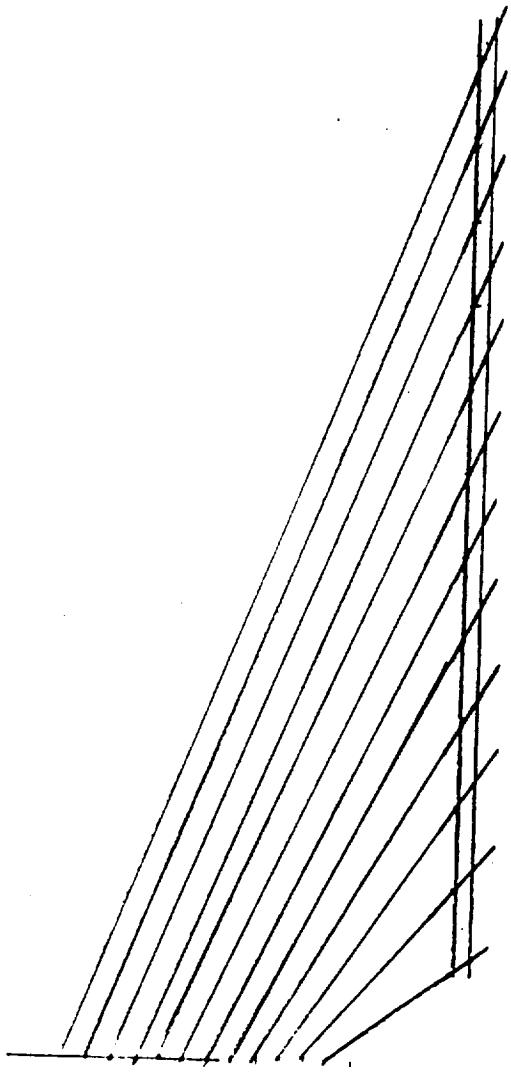

Figure 6. Possible tagging configuration to generate 24 simultaneous velocity measurements.

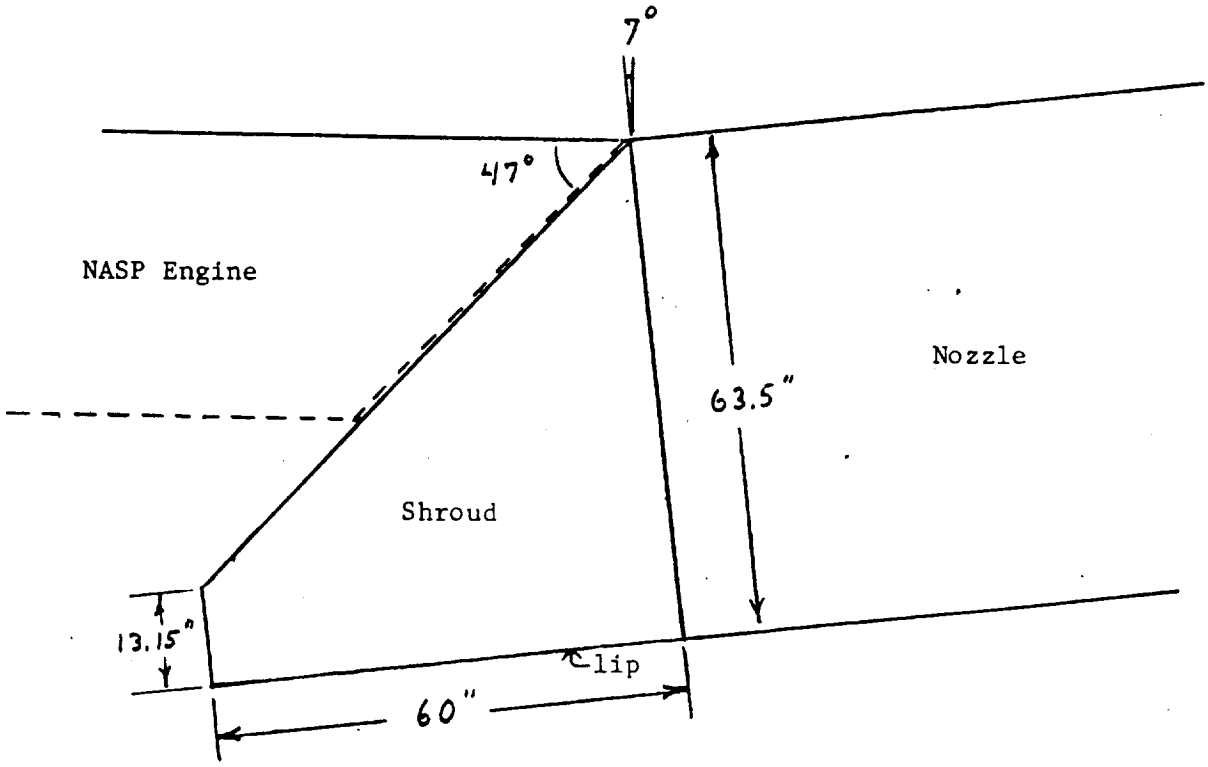

Figure 7. Nozzle exit and shroud geometry.

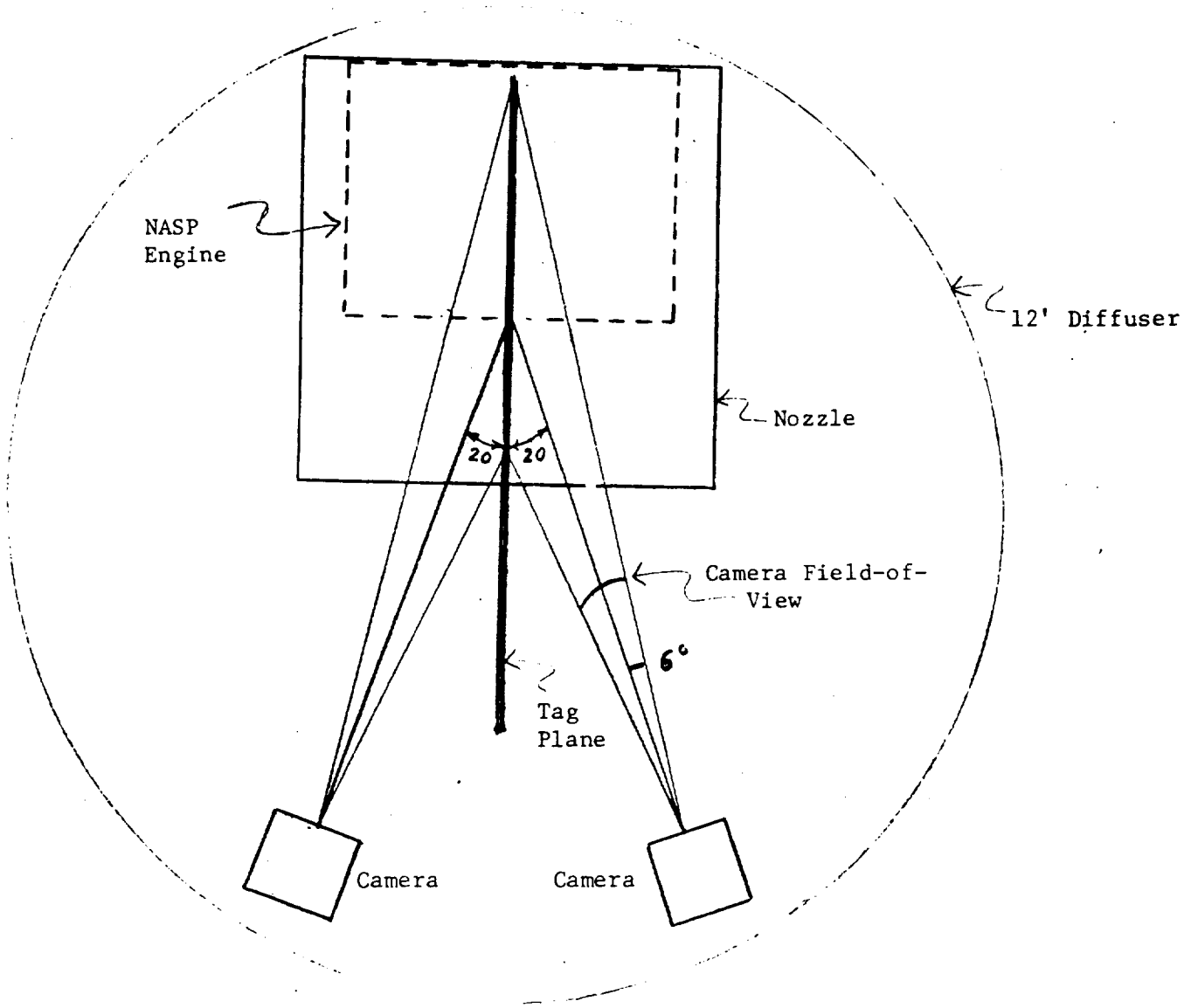

Figure 8. Cross-sectional view of the nozzle exit and diagnostic apparatus.

APPENDIX A
RECOMMENDED VENDOR LIST WITH SPECIFICATION/COST ESTIMATES
FOR ASTF C1 RELIEF VELOCIMETRY INSTRUMENTATION

I. Camera Systems:

ITT Electro-Optics Product Division
3700 E. Pontiac St.
Fort Wayne, IN 46803
219/423-4341
Contact: Richard Hertel

Phase 1 -- Single camera as below:

Description: 40 mm format, dual intensified camera system consisting of intensifier, fiber taper to Cohu CCD array camera, and gatable power supply.

Specifications:

1) 40 mm F4150 Dual Microchannel Plate Intensifier

   a. S-20 spectral response
   b. 20 line pairs/mm resolution
   c. 10^6 luminous gain

2) Cohu CCD Camera

3) Intensifier Power Supply: min 200 nsec Off-On-Off gate duration.

Approximate Cost: $40 K

Phase 2/3: Additional camera as above or 75 mm format camera depending on outcome of laboratory test results.

II. Tunable ArF Interrogation Laser:

Lambda-Physik
289 Great Road
Acton, MA 01720
800/262-1100
Contact: Ron Schaefer

Phase 1:

Description: LPX-150 Tunable Excimer Laser System

Specifications:

1) Series 100 oscillator/Series 200 amplifier
2) 150-200 mJ/pulse @193 nm, 15 Hz
3) Linewidth approximately 1 cm^{-1}
4) Pulse duration: 15 nsec
5) Trigger jitter: 2 nsec
6) Minimum trigger delay: 2 sec.

Approximate Cost: $160,000

Phase 2/3:

Description: Same as above plus Series 200 pre-amplifier and Series 300 final amplifier.

Specifications: 1.3 Joules/pulse @193 nm, 15 Hz.

Approximate Cost: $310,000

Alternate: Phase 1 System and Series 300 amplifier only.

Specifications: 800 mJ/pulse @193 nm, 15 Hz

Approximate Cost: $242,000

III. Mode-Locked Nd:YAG Tagging Laser

Continuum
3150 Central Expressway
Santa Clara, CA 95052
408/727-3240
Contact: John Black
East Cost: David Kemp
508/624-4454

Phase 1:

Description: Active/Active/Passive Mode-Locked Nd:YAG Laser System

Specifications:

1) Pulse duration: 100 psec
2) Pulse energy: 150 mJ @ 1.06 microns, 15 Hz
3) Maximum Repetition Rate: 20 Hz
4) Line width: 1 cm^{-1}
5) Jitter: <25 nsec

Cost: $110 K

Phase 2/3

Description: High power picosecond oscillator/amplifier, Nd:YAG laser system: the size of the system depends on laboratory test results.

IV. Lens Systems

Nye Optical Co.
8781 Troy Street
Spring Valley, CA 92077
619/466-2200
Contact: Richard Nye

Phase 1:

Description: 150 mm f/1.4 lens system.

Specifications:

1) Spectral Transmission: MgF_2 protected UV enhanced aluminum.
   Spectral range: 1800 A to 4.5 microns
2) Angular field: 16^{o}
3) Resolution: 35 line pairs/mm

Cost: $4,100

Phase 2/3: Depends on laboratory test results.

V. Window Materials

Heraeus Amersil, Inc.
650 Jernees Mill Road
Sayreville, NJ 08872
201/254-2500
Contact: Al Kreutzer

Suggested window material is Suprasil-Z fused silica. Available in large variety of standard sizes. Custom windows manufactured on request.

III. PERSONNEL SUPPORTED

A. Principal Investigator: Prof. Richard B. Miles
Princeton University

B. Co-Principal Investigator: Dr. Walter R. Lempert
Princeton University

C. Visiting Scientist: Dr. Ivan Glesk
Mathematics and Physics Faculty
Comenius University
Mlynska dolina F2
84225 BRATISLAVA
Czechoslovakia

D. Research Associate: Dr. Thomas Kreutz
Princeton University

E. Graduate Students:

Barry Zhang
Vinod Kumar
Glenn Diskin

IV. PUBLICATION LIST:

A. Refereed Journals

1. R. Miles and W. Lempert, "Two=Dimensional Measurement of Density, Velocity, and Temperature of Turbulent Air Flows from UV Rayleigh Scattering," Applied Physics B B51, July 1990, p. 1.

2. W.R. Lempert, G. Diskin, V. Kumar, I. Glesk, and R. Miles, "Two-Dimensional Imaging of Molecular Hydrogen in H_2/Air Diffusion Flames Using Two-Photon Laser-Induced Fluorescence," Optics Letters 16, 1991, p. 660.

B. Published Conference Proceedings

1. G.S. Diskin, W.R. Lempert, and R.B. Miles, "Species and Velocity Visualization of Unseeded Heated Air and Combusting Hydrogen Jets Using Laser and Flashlamp Sources," AIAA 26th Joint Propulsion Conference, Paper #AIAA 90-1849, Orlando, Florida, July 16-18, 1990.

2. R.B. Miles and W.R. Lempert, "Velocity and Density Fields in Turbulent Unseeded Air," Fifth International Symposium on Applications of Laser Techniques to Fluid Mechanics, Lisbon, Portugal, July 1990.

3. W. Lempert, B. Zhang, and R. Miles, "A Single Laser Apparatus for Writing Patterns into Unseeded Air," ICALEO'90, November 4-9, 1990, Boston, MA

4. W. Lempert, B. Zhang, G. Diskin, and R. Miles, "Simplifications of the RELIEF Flow Tagging System for Laboratory Use," AIAA 29th Aerospace Sciences Meeting, January 7-10, 1991, Reno, Nevada.

5. G. Diskin, W. Lempert, V. Kumar, I. Glesk, and R. Miles,"Species Imaging in Combusting Hydrogen Jets by Single and Two-Photon Fluorescence and Rayleigh Scattering with Laser and Flashlamp Sources," AIAA 29th Aerospace Sciences Meeting, Jan 7-10, 1991, Reno, Nevada.